Sigma-1 Receptors Modulate NMDA Receptor Function

By:

Alexandra Sokolovski

This thesis is submitted as a partial fulfillment of the M.Sc.

program in Neuroscience

January 10, 2013

Department of Neuroscience
Faculty of Medicine
University of Ottawa

Abstract

The sigma-1 receptor (σ-1R) is an endoplasmic reticulum (ER) protein that modulates a number of ion channels. It is hypothesized that σ-1Rs activated with agonist translocate to the plasma membrane. The σ-1R potentiates *N*-methyl-D-aspartate Receptors (NMDARs), important constituents of synaptic plasticity. NMDARs are anchored in the plasma membrane by Postsynaptic Density Protein-95 (PSD-95). The mechanism behind σ-1R modulation of NMDARs is not known. The results of my investigation confirm that σ-1Rs localize extrasomatically. Following σ-1R activation, σ-1R localization to dendrites and postsynaptic densities (PSDs) is upregulated. Unpublished work from our lab has shown that σ-1Rs associate with PSD-95 and NMDARs. Furthermore, immunocytochemistry (ICC) showed σ-1R colocalization with PSD-95 and NMDAR subunits. After σ-1R activation there was significantly increased colocalization between σ-1R, PSD-95, and GluN2B. Overall, this study may have provided insight into the molecular mechanism behind σ-1R modulation of NMDARs, which could have implications in the understanding of synaptic plasticity.

Table of Contents

List of Tables

List of Figures

List of Abbreviations

σ-1R	sigma-1 Receptor
A647	Alexa-647
ALS	Amyotrophic Lateral Sclerosis
AMPAR	α-amino-3-hydroxy-5-methyl-4-isoxazolepropionic acid receptor
BSA	Bovine Serum Albumin
Ch	Channel
Co-IP	Co-immunoprecipitation
Ctrl	Control
DACk	Donkey Anti-Chicken
DAG	Donkey Anti-Goat
DAMs	Donkey Anti-Mouse
DARb	Donkey Anti-Rabbit
DHEA	Dehydroepiandrosterone
DIV	Days *In Vitro*
eGFP	Enhanced Green Fluorescent Protein
EM	Electron Microscopy
ER	Endoplasmic Reticulum
GFAP	Glial Fibrillary Accessory Protein
HEK	Human Embryonic Kidney
ICA	Intensity Correlation Analysis
ICC	Immunocytochemistry
ICQ	Intensity Correlation Quotient

IHC	Immunohistochemistry
IP3Rs	Inositol 1,4,5-Trisphosphate receptors
MAP-2	Microtubule-Associated Protein 2
Min	Minute
NeuN	Neuronal Nuclei
NH_4Cl	Ammonium chloride
NMDA	*N*-methyl-D-aspartate
NMDAR	*N*-methyl-D-aspartate Receptor
PBS	Phosphate Buffer Saline
PBSGT	PBS with Fish Skin Gelatin and Triton X-100
PFA	Paraformaldehyde
PSD	Postsynaptic Density
PSD-93	Postsynaptic Density Protein 93
PSD-95	Postsynaptic Density Protein 95
SDS	Sodium Dodecyl Sulfate
SEM	Standard Error of the Mean
SK	Ca^{2+}-dependent K^+
SKF	(+)-SKF-10,047
VGCCs	Voltage Gated Calcium Channels

Acknowledgements

First, and foremost I would like to express my sincere gratitude to my supervisor, Dr. Richard Bergeron, for providing me with the opportunity to pursue a Master's degree in his lab and allowing me to study the wonderful story of the σ-1 receptor. His encouragement and understanding throughout the years have been of great value to me. I would like to thank my committee members Dr. Johnny Ngsee and Dr. Diane Lagace for their insights and suggestions over the years, which have helped me improve as a scientist. I would also like to thank my mentors Mohan Pabba and Dr. Adrian Wong for helping me throughout the past three years since I first joined this lab. Their patience, questions, and thought provoking discussions have allowed me to continually improve over the years and become more independent. I would like to thank our lab manager Nina Ahlskog for answering my countless questions over the years, and the rest of the Bergeron lab for the many helpful discussions that were provided that improved me as a scientist and critical thinker. I would also like to thank Dr. Jean-Claude Beique's lab, in particular Ling Tian who has helped me with dissociated neuron cultures and molecular biology techniques, as well as Cary Soares and Kevin Lee for letting me take over their microscope in the past year and having the patience to answer my many questions.

I would also like to thank my family and friends, especially my parents Irina Sokolovski and Genadi Makhlin, and boyfriend Philippe Aubry-Boyle, for continually supporting and encouraging me in all of my endeavors.

1. Introduction

1.1. Preface

Most, if not all, ion channels are known to undergo some form of modulation to enhance or reduce the flow of ions across a membrane[1]. Ion channel modulation is an important component of synaptic plasticity and allows neurons to adapt to changes in their environment[2]. The sigma-1 receptor (σ-1R) is a unique endoplasmic reticulum (ER) protein that binds a wide range of ligands[3], and participates in an assortment of cellular processes, including neuroplasticity[4] and cognitive function[5]. Its capacity to be involved in a variety of cellular processes likely stems from its role in modulating an extensive number of voltage-gated ion channels ranging from Na^+ channels[6] to voltage-gated Ca^{2+} channels (VGCCs)[51]. σ-1Rs also regulate the ligand-gated *N*-methyl-D-aspartate Receptor (NMDAR)[7], a key initiator of several forms of synaptic plasticity[8]. Therefore understanding the molecular mechanism behind σ -1R modulation of ion channels could have implications in the understanding of synaptic modifications.

1.2. σ -1R Discovery and Characterization

In 1976 Martin, et al. classified three opioid receptors based on pharmacology, one of which was the opioid receptor[9]. The σ/opioid receptor was responsive to SKF-10,047 and blocked by administration of opioid antagonist naloxone. In 1982 the σ/non-opioid receptor was identified, one which was not responsive to the opioid antagonist naloxone[10]. Based on ligand binding assays two subtypes were proposed: σ-1 and σ-2 receptors[11]. While the σ-1R is fairly well characterized, little is known about the σ-2 receptor.

As the σ-1R does not have homologous proteins in the mammalian system, it was difficult to characterize the receptor. A large breakthrough occurred in the field in 1996 with the cloning of the σ-1R from guinea pig liver[12]. Subsequently, σ-1R sequences were cloned in the murine[13], human[14], and rat[15] systems with greater than 80% homology to the original guinea pig sequence. It is now known that the σ-1R is composed of 223 amino acids, and a molecular weight of 23 to 25kDa[12-15]. While the crystal structure of the σ-1R has not been determined, it is believed to have three hydrophobic domains (at the N- and C-termini, and center)[12], two of which are transmembrane (near N-terminus and center) (**Figure 1**)[16], with the C- and N-termini localizing to the lumen of the ER[16]. Amino acids on the C-terminus and second transmembrane domain are responsible for ligand binding[13,17,18].

1.3. σ -1 Receptor Localization

σ -1Rs are ubiquitously expressed throughout the body[15], including the central nervous system. With the use of radioligand binding assays, immunohistochemistry (IHC), and electron microscopy (EM) σ -1R expression has been shown in the hippocampus, cortex, cerebellum, hypothalamus, brainstem, and spinal cord[19,20].

σ -1R immunoreactivity can be detected in neurons and glia, including astrocytes[21], oligodendrocytes[22], and Schwann cells[23]. At the subcellular level the σ-1R is primarily detected in perikarya[19]. σ-1Rs preferentially localize to the ER near mitochondrial membranes, referred to as the Mitochondrial-Associated Membranes (MAM)[24]. They also localize to nuclear envelopes, and ER globular protrusions[20,21]. EM studies demonstrate that σ-1Rs localize to dendrites and postsynaptic terminals[19,20]. However postsynaptic localization of σ-1Rs is still debated as the peroxidase stain is difficult to differentiate

from the postsynaptic density (PSD). Notably, σ-1Rs have not been detected on presynaptic terminals[19].

1.4. σ -1 Receptor Pharmacology

Radioligand binding assays indicate that σ-1Rs bind to an extensive number of ligands (**Table 1**). The receptor was first identified through benzomorphan affinity assays for opioid receptors. Unlike opioid receptors which have a preference for levorotatory benzomorphans, the σ-1R has a preference for dextrorotatory enantiomers[10]. Commonly used benzomorphans with high affinity for the σ-1R are the σ-1R agonists (+)-SKF-10,047 (SKF) and (+)-pentazocine. Many σ-1R ligands are derivatives of benzomorphans, with similar structures (**Figure 2**). σ-1R ligands with benzomorphan skeletons include, antipsychotics, SSRIs, and neurosteroids.

Most antipsychotics, with the exception of atypical antipsychotics, have high to medium binding affinities to the σ-1R[25-27]. This includes imipramine, chlorpromazine, and pimozide[10]. Furthermore, some SSRIs have high to moderate affinity for σ-1Rs[28]. It is not known if all ligands that bind σ-1Rs *in vitro* have an effect *in vivo*, as they may not reach high enough levels in the vicinity of the σ-1R ligand-binding domain to produce an effect.

σ-1R ligands innate to the mammalian system have also been detected. The neurosteroid progesterone has the highest affinity for the σ-1R, followed by testosterone, androsterone, and deoxycorticosterone[29], which have moderate binding affinities for the σ-1R. Pregnonolone sulfate and dehydroepiandrosterone (DHEA) have weaker affinities for the σ-1R[29,30]. When administered to animals, pregnenolone sulfate[31], DHEA[31], and progesterone[32] induce behavioral actions related to learning and memory via the σ-1R[33].

However, it has not been confirmed which of these ligands function on the σ-1R endogenously.

1.5. σ -1R Function

σ-1Rs modulate ion channels involved in processes such as regulation of resting membrane potentials, action potentials, and synaptic modifications. Nevertheless, knockout of σ-1Rs is nonlethal, with mice showing no overt phenotypic differences from wildtype mice[34]. The spatial working memory was examined using spontaneous alteration response in a Y-maze[35]. While male σ-1R knockout mice were not significantly different from wildtype, female σ-1R knockout mice showed impairment in spatial memory. This deficit increased with age, and could be reversed by supplementing the mice with 17β-estradiol dehydrogenase, which showed lower expression levels in σ-1R knockout mice. This signifies an indirect action through σ-1Rs. No change was observed in contextual long-term memory which was analyzed using the step-through avoidance response[35]. Using place-learning ability in the water-maze, female σ-1R knockout mice were shown to have impaired spatial long-term memory, which was also recovered to wildtype levels through administration of 17β-estradiol dehydrogenase. Male σ-1R knockout mice showed increased response to anxiety, shown through their decreased time spent in the center of an open-field, increased latency to enter the dark compartment during passive avoidance testing, and decreased time spent in the open arms of the elevated plus-maze[35]. Acute knockdown of σ-1Rs causes inhibition of oligodendrocyte differentiation[21], decreases cancer cell proliferation[36], and decreases formation of dendritic spines in hippocampal neurons[37].

The σ -1R regulates a number of neurotransmitter systems. This includes the glutamatergic[38,39], dopaminergic[40], serotonergic[41], norepinephrine[42], and cholinergic systems[43]. Its ability to regulate so many different neurotransmitter systems stems from the receptor's role in modulating a wide range of ion channels postsynaptically (**Figure 3**), and neurotransmitter release presynaptically. The σ-1R regulates voltage-gated ion channels, which include K^+ channels[16,44-47], Na^+ channels[6,48], and VGCCs[51,52,49,50]. σ-1Rs also modulate the ligand-gated inositol 1,4,5-trisphosphate receptors (IP3Rs)[5119,36] and NMDARs[7].

σ -1Rs modulate ion channels and presynaptic release through two mechanisms. The first is through cell signaling pathways involving G-proteins[39,44,48,52,53]. The second is through direct interactions with ion channels[16,24,50]. It is hypothesized that σ -1Rs translocate from the ER to the plasma membrane where the interaction between σ -1Rs and ion channels might occur, although this still needs to be established. It is important to note that σ-1R ligands show no pharmacological function via the σ -1R unless there is simultaneous activation of the ion channel that σ-1R is to modulate. For example, in experiments performed to potentiate NMDARs, postsynaptic currents need to be evoked in conjunction with σ-1R agonist in order to achieve potentiation of NMDARs. Despite the modulatory nature of σ-1Rs, immunocytochemistry (ICC) shows that the receptor translocates from the cytoplasm towards the plasma membrane after application of agonist (+)-pentazocine[54].

1.5.1. Presynaptic Actions of σ-1R

σ-1Rs are able to up-regulate presynaptic release in several neurotransmitter systems. σ-1R agonists potentiate acetylcholine release in the frontal cortex and hippocampus[55].

They also modulate NMDAR-dependent release of norepinephrine in hippocampal slices, which occurs through a G-protein mechanism with σ-1R agonists potentiating release of norepinephrine[52]. In cultured hippocampal neurons σ-1R agonist pregnenolone sulfate increases spontaneous presynaptic glutamate release through σ-1Rs and G-proteins[39].

The σ-1R is also involved in inhibition of neurotransmitter release. In rat striatal slices σ-1R inhibits NMDAR-dependent dopamine release through a PKC-dependent pathway[56]. Furthermore, administration of σ-1R agonist results in inhibition of presynaptic glutamate release in the cortex[38]. This is dependent on PKC activation and entry of Ca^{2+} through VGCCs[38]. Lastly, σ-1R activation in inhibitory neurons of the hippocampus results in inhibition of GABA release through a G-protein mechanism[53], possibly contributing to modulating background excitability and allowing long-term potentiation[57].

1.5.2. σ-1R Modulation of Ion Channels: IP3Rs

IP3Rs reside on the ER and allow for Ca^{2+} diffusion from intracellular stores[51]. They are inhibited under basal conditions through a direct association with the cytoskeletal protein ankyrin[19,36]. Su et al.[24] has shown that in its dormant state, the σ-1R resides in the ER bound to binding immunoglobulin protein (BiP). σ-1R activation by ER stress leads to its dissociation from BiP and formation of a complex with IP3Rs via the σ-1R C-terminus at the MAM (Figure 3)[19,36]. The formation of a complex between σ-1Rs and IP3Rs results in stabilization of the active IP3R at the ER membrane, and subsequent increased ion flow through IP3Rs[19].

1.5.3. σ-1R Modulation of Ion Channels: K^+ Channels

K^+ channels are crucial in shaping action potentials and resting membrane potentials through diffusion of K^+ out of the cell along the electrochemical gradient[58]. As a result, their inhibition yields decreased neuron excitability[45]. Electrophysiology experiments have demonstrated that σ-1Rs negatively modulate a variety of K^+ channel subtypes through G-protein dependent and independent methods (**Figure 3**)[16,44-47]. In cultured melanotrope cells σ-1R agonists decrease the transient A-type K^+ current through G-protein signal transduction[44]. Whereas delayed outward rectifying K^+ channels[45], Ca^{2+}-dependent K^+ (SK) channels[46], and A-type K^+ channels[16] in oocytes are all blocked by σ-1R activation through a G-protein independent mechanism. This suggests a direct coupling between σ-1Rs and some K^+ channel subtypes[47]. Further supporting this are co-immunoprecipitation (co-IP) assays that show σ-1Rs form a complex with the A-type K^+ channel in rat tissue. Therefore it is hypothesized that σ-1Rs act as auxiliary subunits to voltage-gated K^+ channels[16,46,47]. It is not known which part of the σ-1R sequence binds K^+ channels[16].

1.5.4. σ-1R Modulation of Ion Channels: Na^+ Channels

Na^+ channels allow for the diffusion of Na^+ into the cell along a neuron's chemical gradient, which is associated with the rising phase of an action potential[58]. σ-1R inhibition of Na^+ channels results in decreased action potential initiation and amplitude[6]. In cortical slices, σ-1R agonists inhibit persistent Na^+ currents, which play a role in setting the membrane potential[48]. This effect is reversed with G protein inhibitors and PKC inhibitors[48]. Therefore the modulation of persistent Na^+ currents occurs through a G protein and PKC dependent mechanism.

1.5.5. σ-1R Modulation of Ion Channels: VGCCs

VGCCs are plasma membrane ion channels that permit diffusion of extracellular Ca^{2+}into the cell, a requirement for presynaptic release of vesicles, electrical activity (i.e. Ca^{2+} spikes), and cell signaling mechanisms[59,60]. In dissociated neuron cultures σ-1R ligands block all VGCC subtypes: N-, L, P/Q, and R-type[61,62]. Tchedre, et al. show that in retinal ganglion cells the activated σ-1R forms a complex with L-type Ca^{2+}channels[50]. However, no effect is seen on Ca^{2+} influx through VGCCs *in vivo* when σ-1R ligands are administered to wildtype and σ-1R knockout mice[49].

1.5.6. σ-1R Modulation of Ion Channels: NMDARs

The NMDAR is the only ligand-gated plasma membrane channel regulated by the σ-1R[7]. NMDARs are glutamate-gated ion channels that allow for diffusion of Na^{+}, K^{+}, and Ca^{2+} across the plasma membrane[63]. They consist of four subunits, including two obligatory GluN1 subunits[63], and two GluN2(A-D)[64] or GluN3(A-B) [61] subunits. As NMDARs permit Ca^{2+} diffusion into neurons, postsynaptically they play a central role in cellular signaling and promoting the modification of synapses[8,65]. Synaptic modifications that can be triggered by NMDARs include Long-Term Depression and Long-Term Potentiation (LTP), which are molecular determinants of learning and memory[66].

σ-1Rs potentiate NMDARs through application of σ-1R specific agonists[7]. This potentiation can occur through either a modification of gating properties, or an increase in trafficking or retention in the plasma membrane. The molecular mechanism behind σ-1R modulation of NMDARs has not been determined, however it must occur through either a signaling mechanism or a direct interaction. Martina, et al proposed that it might occur through an SK-mediated method[67]. In this case the inhibition of SK channels shunts

NMDAR responses[67], as SK channels are known to inhibit NMDAR currents[68]. Conversely, if σ-1R modulates NMDARs through a direct interaction, the two proteins might form a complex, possibly requiring an intermediary protein. Possible candidates for NMDAR plasma membrane retention are membrane-associated guanylate kinases, such as Postsynaptic Density Protein 95 (PSD-95) or Postsynaptic Density Protein 93 (PSD-93), which are known to maintain NMDARs within the plasma membrane of the PSD and dendrites[69,70]. *In vitro* systems suggest that the relationship between NMDARs and PSD-95 is important for synaptic function[69,71].

σ-1R ligands are believed to have a behavioral effect in animals through modulation of NDMARs, as animal models of amnesia treated with σ-1R ligand show improved learning and memory, a common phenotype associated with NMDAR function[5,72]. Furthermore, chronic administration of DHEA in rats facilitates the induction of LTP in synapses through an NMDAR-dependent mechanism[4].

2. Working Hypothesis

Based on the information provided thus far in the literature I made three hypotheses. The first is that based on the state of current literature I expected to find σ-1R localization to cell bodies, dendrites, and PSDs in the absence of σ-1R activation in pyramidal neurons of the hippocampus and dissociated neuron cultures. Secondly, activation of σ-1Rs would lead to increased localization of σ-1Rs in dendrites and PSDs. Lastly, activation of σ-1Rs would result in increased colocalization between σ-1Rs, NMDARs, and PSD-95 in dendrites and PSDs.

3. Aims

My first aim was to perform an in depth study of σ-1R localization to dendrites and synaptic terminals in hippocampal slices and dissociated cortical cultures. The hippocampus was selected as σ-1R expression[19] and σ-1R potentiation of NMDARs[7] have been previously demonstrated. σ-1R localization was predominantly assessed at dendrites and synaptic terminals, as the main interest of this study was to gain an understanding of the molecular mechanisms behind σ-1R ion channel modulation.

My second aim was to show that σ-1Rs translocate to dendrites and PSDs after activation with an agonist. It has not previously been shown which compartment the σ-1R translocates to after activation in neurons. Therefore colocalization studies with dendritic and synaptic terminal markers were performed after treatment with σ-1R agonist SKF. Based on previous findings I did not expect presynaptic localization of σ-1Rs[19].

To assess if σ-1Rs might potentiate NMDARs through a direct mechanism, my third aim was to assess colocalization between σ-1Rs and NMDARs before and after σ-1R activation. Unpublished work from our lab suggested a link between the σ-1R, NMDAR, and PSD-95. Therefore I expected to see an increase in colocalization of σ-1Rs with PSD-95 and NMDAR subunits after σ-1R activation with SKF. This is the first study in which the mechanism and location of interaction between σ -1Rs and NMDARs has been investigated.

This study will assist in understanding the mechanism behind σ-1R modulation of ion channels by determining if σ-1R activation results in its upregulation in dendrites and PSDs, where NMDARs localize. It is rare for a single protein to be involved in the modulation of so many different systems. In order to gain a better understanding of the

molecular mechanisms underlying synaptic modifications, it is important to learn the mechanism behind σ-1R modulation of NMDARs, a protein implicated in the initiation of synaptic plasticity.

4. Materials and Methods

4.1 Ethics Approval

Male Sprague Dawley rats were housed in a temperature and humidity controlled environment, with 12 hour light/dark cycles. Animals had constant access to food and water. Anesthesia and surgical protocols were performed in accordance with approved University of Ottawa Animal Care and Use Protocols.

4.2. Banker Cultures

4.2.1. Astrocyte Isolation

Astrocytes were isolated according to the protocol by Kaech and Banker[73], with minor modifications. Three P1 rats were sacrificed and the brains removed into ice-cold choline cutting solution (119mM choline chloride, 2.5mM KCl, 4.3mM $MgSO_4$-$7H_2O$, 1mM $CaCl_2$, 1mM NaH_2PO_4-H_2O, 1.3mM ascorbic acid, 11mM glucose, $NaHCO_3$, 1mM Kynurenic Acid). In a laminar flow hood with the use of a dissecting microscope the cerebral hemispheres were dissected out and meninges removed. Cerebral hemispheres were transferred to a drop of choline cutting solution and cut into small pieces with scissors. The tissue was transferred into choline-cutting solution containing 0.6mg/mL papain and 0.1% DNase I. Tissue was incubated at 37°C for 10 minutes with occasional swirling. It was then passed through a 10mL pipette 10-15 times, followed by another incubation for 10 minutes at 37°C. Tissue was pipetted up and down a 5mL pipette 10-15 times until most chunks disappeared. The cell suspension was passed through a cell strainer to remove residual chunks and collected in glial media. Cells were centrifuged at 400g for five minutes. The cell pellet was resuspended in glial media and cells were

plated at $7.5x10^5$ cells per $75cm^2$ flask in glial media. The next day culture media was changed with a brief rinse and addition of fresh glial media. From then on the cultures have a media change every three days, progenitors and microglia were dislodged by hitting the flask before media changes. At the time of experiment Banker cultures were predominantly composed of astroglia (~90%), with a small proportion of oligodendrocytes (~10%).

4.2.2. Preparation for Neuronal Isolation

One week before plating neurons for banker cultures, astroglia were harvested, resuspended in glial media, and plated in 12-well plates at a density of 10^5 cells per dish. One or two days before neuron isolation, glial media in 12-well plates was replaced with neuronal maintenance medium for conditioning. The day before plating neurons wax dots, prepared by melting paraffin, were applied to coverslips followed by 2mg/mL poly-lysine in borate buffer and coverslips were placed in a 37°C incubator overnight. The morning of plating the poly-lysine was thoroughly washed off and neuronal plating media was applied.

4.2.3. Neuron Isolation

A pregnant dam was sacrificed and the uterus dissected out. In a laminar flow hood the fetuses were removed, brains dissected out, and placed in ice-cold choline cutting solution. With a dissecting microscope meninges were removed from the cerebral hemispheres and the cortex dissected out. All cortices were placed in choline cutting solution containing 0.9mg/mL papain. Tissue was incubated at 37°C for 15 minutes. Papain solution was substituted with choline cutting solution and the brains were incubated for five minutes at room temperature. This was done twice to remove all

papain, and the final volume was brought to 2-3mL. Hippocampi were dissociated by repeatedly pipetting up and down with a Pasteur pipette beginning with 5-10 passes through a regular pipette, followed by two successively smaller pipettes. Neurons were plate at a density of $1x10^5$ cells/cm^2 for Banker cultures, $4x10^5$ cells/cm^2 for low-density cultures, and $1.2x10^6$ cells/cm^2 for high-density cultures used for transfections. After 3-4 hours the coverslips with paraffin feet (Banker Cultures only) were flipped upside down in glial dishes so paraffin feet were resting on the bottom of the dish, and the cultures were fed once per week by removing one-third of the media and replacing with fresh neuronal maintenance media.

4.2.4. Lipofectamine Transfection of Neuron Cultures and Live Imaging

Lipofectamine (Invitrogen) was used to transfect neuronal cultures as per manufactured instructions (Invitrogen). Neuronal cultures were transfected with a C-terminus YFP-tagged σ-1R in a pEYFP-N1 vector (gift from Dr. Tsung Ping Su) and mCherry-C1. 3μL Lipofectamine per well was added to DMEM, and in a separate Eppendorf tube a total of 1μg DNA per well (0.7μg σ-1R-YFP and 0.3μg mCherry) was added to DMEM. After five minutes, the two tubes were mixed together, and incubated for 15 minutes. 900uL of preheated neuronal incubation media (1X MEM, 1X glutamax, 20mM HEPES, 1mM Na^+ pyruvate, 35mM glucose) was added to each well of a 12-well plate. 100uL of lipofectamine solution to each coverslip-containing well drop-wise. Coverslips were incubated in CO_2-free conditions at 37°C for one hour, and placed in to the 37°C incubator with 5% CO_2 for 24-36 hours before imaging.

4.2.5. HEK Cell Maintenance and Transfection

Human Embryonic Kidney (HEK) cells were kept in a 37°C incubator in maintenance media (MEM, 1X glutamax, 1X penicillin-streptomycin, 10% fetal bovine serum), and harvested twice per week once the confluency reached ~80-90%. Transfections were performed with TransIT Transfection Reagent (Mirus) following manufacturer instructions. HEK cells were transfected with PSD-95 in an eGFP-N1 vector. TransIT was added to MEM (Invitrogen) in an Eppendorf tube. 1μg DNA was added to MEM in a separate Eppendorf tube. After five minutes, the two tubes were mixed together, and incubated for 20 minutes. 100uL of TransIT-DNA solution was added to each well of a 12-well plate dropwise. Coverslips were incubated at 37°C for two hours, and media was replaced with fresh HEK cell media with AP5.

4.3. Immunofluorescence

4.3.1. Fixation and Slice Preparation

Previous *in vivo* studies performed in the lab showed an association between σ-1Rs and NMDARs (Figure 13) after a 90-minute treatment with SKF. For animals treated with σ-1R agonist, Male Sprague Dawley rats were given an injection of 1mg/kg SKF (Tocris) in Phosphate Buffer Saline (PBS) intraperitoneally 90 minutes prior to fixation. Rats were given an overdose of pentobarbital (150mg/kg) via intraperitoneal injection. An intracardiac perfusion was performed through the left ventricle beginning with 60mL of heparin (10U/mL, pH 7.4) in PBS and followed by 60mL of paraformaldehyde (PFA) (4%, pH 7.4) in 1X PBS given over approximately five minutes. The forebrain and hindbrain were discarded, and the remainder of the brain post-fixed in the same solution for 24 hours. Successive sucrose incubations were performed from 10% to 30% over a

three-four day period. Brains were frozen in -35°C Celsius isopentane, embedded in Shandon Cryomatrix (Thermo Scientific), and stored in the -80°C Celsius freezer until cutting of 10μm sections at -30°C using a cryostat (Leica).

4.3.2. IHC

Slices were postfixed for five minutes in PFA (4%, Sigma) in 1X PBS, and the remaining PFA was quenched with ammonium chloride (NH_4Cl) (50mM, pH 7.4, Sigma) in 1X PBS for 30 minutes. Antigen retrieval was performed for five minutes with Sodium Dodecyl Sulfate (SDS) (0.2% SDS, BioShop) in 1X PBS. Blocking was carried out in PBS with fish skin gelatin and Triton X-100 (0.25% fish skin gelatin (Sigma) and 0.2% Triton X-100 (Sigma) in 1X PBS, pH7.4) for 45 minutes. This was followed by incubation in primary antibodies (Table 1) in bovine serum albumin (BSA) (1%, Sigma) in 1X PBS overnight at 4°C. Sections were washed three times with PBSGT for five minutes each, and incubated in secondary antibodies for two hours. A final three-five minute washes were carried out with PBSGT, and slides were mounted with Vectashield (Vector Labs) for immunofluorescence.

4.3.3. ICC – Neuron Cultures

For cultures that were treated with agonist, 1μM SKF was maintained in the media for 15-45 minutes. For controls, 100μM of σ-1R antagonist BD-1047 was added to the cell media 2-3 hours prior to a 30-minute incubation with SKF. Cells, at 14 days *in vitro* (DIV), were fixed with PFA (4%) in 1X PBS for 10 minutes. Excess PFA was quenched with 50mM NH_4Cl, followed by a postfixation with ice-cold methanol (Sigma) at -20°C for five minutes. Coverslips were then permeabilized with Triton X-100 (0.2%) in 1X PBS for ten minutes, blocked with fish skin gelatin (0.25%) in 1X PBS, and incubated

overnight in primary antibody at 4°C (**Table 2**). Coverslips were rinsed with 0.01% Triton X-100 (0.01% in 1X PBS) three times for five minutes, followed by incubation in secondary antibody for two hours, and a final three-five minute rinses in PBST. Coverslips were mounted on glass slides with Vectashield.

4.3.4 ICC – HEK Cells

Cells were fixed with 4% PFA for 20 minutes, and remaining PFA was quenched with 50mM NH_4Cl for 30 minutes. Cells were blocked and permeabilized in PBSGT, followed by an overnight incubation in primary antibody in PBSGT at 4°C. Three washes of five-minutes each were performed, with PBSGT. Secondary antibody was incubated for 2 hours, followed by another set of three-five minute washes. Coverslips were mounted on glass slides with Vectashield.

4.3.5. Imaging

Images were acquired with an Olympus confocal microscope system using the following laser wavelengths: 488nm, 559nm, and 635nm. To avoid crosstalk the multi-track configuration was used. The following filters were used to collect emission from CY3, Alexa-647, and FITC: BA575-620, BA655-755, and BA505-540.

High power images in the hippocampus were acquired by centering in the middle of the CA1 at or directly below (<50μm) the cell bodies depending on the cell marker being imaged. For images that were used in colocalization analysis, cell bodies were outside the field of view (<20μm). For dissociated neuron cultures, images used in colocalization analysis were taken in the apical proximal dendrites directly adjacent to the cell body. All images used for colocalization analysis were taken with a Kalman averaging of 3, a saturation of less than 1%, and z-stacks with sections of ~1μm frequency.

For live imaging, coverslips with 17-18 DIV neuron cultures were placed in baths containing HEPES buffer (150mM NaCl, 3mM KCl, 1.3mM $MgCl_2$, 2mM $CaCl_2$, 10mM HEPES, 10mM Glucose, 1.3mM Ascorbic Acid).

4.3.6. Image Analysis

Analysis was performed with ImageJ2 software and Excel. Low magnification images were assembled using the stitching plugin "Stitch Directory with Images (unknown configuration)"[74]. All object-based colocalization analysis was performed with Excel as described below. Intensity Correlation Analysis (ICA) was also performed with Excel with a modification to the original Li method[75]. Costes thresholding in ImageJ2's JaCoP[76] was used to limit background and noise signals[77]. Averages were taken for colocalization findings and standard error of the mean (SEM) calculated. Statistical significance was measured to assess the difference in σ-1R colocalization with markers at different time points using an unpaired two-tailed T-test.

We employed an object-based quantification method[76] as a measure of colocalization (**Figure 4A**). The colocalization was assessed by measuring the number of overlapping pixels in a channel normalized to the sum of pixels in all channels. For an assessment of σ-1R localization to cytoplasm, an ROI was drawn around the lighter section of NeuN stain (**Figure 5B**).

ICA was used to analyze the change in colocalization between σ-1R, NMDAR, and PSD-95 in the absence and presence of SKF treatment. ICA measures the synchrony in pixel intensity variations between two channels by producing a value, Intensity Correlation Quotient (ICQ), between -0.5 and 0.5[75] (**Figure 4B**). The ICQ suggests if the

colocalized pixel intensities are varying in synchrony, aka dependent (~ 0.5), varying asynchronously, aka independently (~ -0.5), or varying randomly (~0).

As this method was limited to analyzing colocalization between two channels at a time, rather than the three required for analysis of σ-1R colocalization with NMDARs and PSD-95, a modification was made to account for all three proteins simultaneously (**Figure 4C**). Initially, the relationship between σ-1R and PSD-95 was measured. For all σ-1R pixels that showed a dependent relationship relative to PSD-95, a comparison was made to the NMDAR channel.

5. Results

5.1. σ-1R Localization

To analyze σ-1R subcellular localization in detail σ-1Rs were costained with various cellular markers. The nuclear marker Neuronal Nuclei (NeuN) shows intense stain in the nucleus and weak stain in cytoplasm[78]. It was used to assess localization to perikarya within the hippocampus. The Glial Fibrillary Acidic Protein (GFAP) was used to identify astrocytic localization of σ-1R[79]. The dendritic marker Microtubule-Associated Protein 2 (MAP-2) was used for dendritic localization of σ-1Rs[80]. Lastly, for synaptic terminal localization postsynaptic protein PSD-95[81], and presynaptic marker synaptophysin[82] were utilized.

At low magnification the overall distribution of hippocampal NeuN stain showed a sideways "U"-shape with an inverted "V"-shaped dentate gyrus (**Figure 5A**)[83]. NeuN displayed strong nuclear and weak cytoplasmic stain (**Figure 5B**), with a stain-free circular region in the nucleus likely corresponding with high chromatin density[78] (**Figure 5B**). GFAP showed characteristic star-shaped cell bodies (**Figure 5C**), and hippocampi showed well-defined dendritic stain when labeled with MAP-2 (**Figure 5D**). PSD-95 and synaptophysin displayed a punctate stain as would be expected for proteins localized to synaptic terminals (**Figure 8J,M**)[84,85].

Controls were prepared by excluding primary antibodies (**Figure 6**). Blank results were obtained for all antibodies with the exception of donkey anti-rabbit (DARb) Alexa-647 in neuron cultures (**Figure 6C**). The Alexa-647 antibody localized exclusively to the nucleus in the absence of primary antibody, where colocalization studies were not performed.

The σ-1R localizes throughout the entire hippocampus (**Figure 7**), with the highest intensity of σ-1R stain in the stratum moleculare, followed by moderate stain in cell bodies. Little stain is detected within the CA4. At the subcellular level, σ-1Rs colocalized with cytoplasmic NeuN (**Figure 8A**). Little colocalization was detected between σ-1Rs and GFAP (**Figure 8D**). σ-1Rs localized to dendrites (**Figure 8G**), PSDs (**Figure 8J**), and presynaptic terminals (**Figure 8M**).

5.2. σ-1R Translocation with Agonist Treatment

Unpublished data from our lab has shown that rats given a 90-minute treatment of σ-1R agonist SKF have increased levels of NMDAR subunits and PSD-95 in synaptosome isolates (**Figure 9**). It is therefore possible that σ-1R forms an association with NMDARs at this time point. To assess if σ-1Rs do in fact translocate to dendrites and PSDs where PSD-95 and NMDARs localize, colocalization between σ-1Rs and cellular markers was measured after a 90-minute treatment with SKF.

While there was an increase in localization to dendrites and presynaptic terminals, overall a statistically significant difference was not detected in σ-1R localization within the various cell compartments. σ-1R colocalization with NeuN did not change in rats treated with SKF (untreated samples (C)=12.8%±1.8%, treated with SKF (**Figure 8B,C**). Also, σ-1R colocalization with GFAP did not change after treatment with SKF (**Figure 8E,F**). σ-1R colocalization with MAP-2 (**Figure 8H,I**) and synaptophysin (**Figure 8N,O**) increased with SKF treatment, however these increases were not statistically significant. Lastly, there was a statistically insignificant decrease in σ-1R colocalization with PSD-95 (**Figure 8K,L**).

5.3. Localization of σ-1Rs in Dissociated Cultures

The main concern with localization studies in slices is the high density of neurons and the resulting difficulty in isolating adjacent cellular compartments. This is especially true in dendritic arborizations where there is little separation between dendrites, and pre- and postsynaptic terminals which might result in them being incompletely differentiated due to resolution limits. Therefore σ-1R localization was also investigated in cortical-dissociated cultures using low density and Banker culturing methods[73]. σ-1R colocalization was measured at proximal apical dendrites, within 20μm of the cell body. Due to the nonspecific staining (Figure 6C) obtained with the secondary antibody used against σ-1R in dissociated neuron cultures, localization of σ-1R to the cell body was not assessed.

Consistent with results found using IHC, σ-1R colocalized with dendritic marker MAP-2 in dissociated cultures (**Figure 10B**). Interestingly, σ-1R clusters aggregate around dendritic branch points (**Figure 10B**), and this point is further emphasized in high-density dissociated neuron cultures transfected with σ-1R-YFP. When σ-1R-YFP was overexpressed in hippocampal cultures, σ-1R puncta could be detected at most branch points in the dendritic arbor (**Figure 10C-D**). Further costaining of σ-1Rs with synaptophysin and PSD-95 showed that σ-1Rs also localized to presynaptic terminals (**Figure 11J,L**), and PSDs (**Figure 11B,D**).

5.4. Translocation of σ-1Rs in Dissociated Cultures

SKF treatment in dissociated cultures resulted in significant increases in σ-1R localization to dendrites and PSDs. As the time required for σ-1R activation after direct application to the cells was not known, a time-course was performed with 15-minute time

points up to 45 minutes. The results observed were quite different from those obtained with IHC (**Figure 11**). There was significantly increased colocalization of σ-1Rs with PSD-95 after 15 ($p<0.05$) and 30 minutes ($p<0.01$) relative to untreated cultures (**Figure 11D**). Interestingly, 45 minutes after σ-1R agonist treatment colocalization between σ-1Rs and PSD-95 decreased back to untreated levels. This is a significant drop from σ-1R localization at PSDs at 30 minutes ($p<0.01$). Controls were performed by pretreating dissociated neuron cultures with 100μM of σ-1R antagonist BD-1047 for two hours prior to incubation with SKF for 30 minutes. The control for σ-1R colocalization with PSD-95 showed levels similar to untreated cultures.

A significant increase was detected for σ-1R localization to dendrites after SKF treatment (**Figure 11F-H**). Colocalization of σ-1R with MAP-2 increased significantly 30 minutes after SKF treatment ($p<0.05$) relative to untreated cells (**Figure 11H**). Compared to the untreated samples, colocalization between σ-1R and MAP-2 did not change much after 15-minutes of SKF treatment. After 45 minutes the dendritic localization decreased relative to the 30-minute time-point, however it was statistically insignificant. The control pretreated with BD-1047 showed similar levels to the untreated cultures.

σ-1R localization to presynaptic terminals increased after SKF treatment, however cell-to-cell variation was too large to produce statistical significance in this case (**Figure 11I-K**). There was no significant change in colocalization of σ-1R and synaptophysin after 15 minutes of SKF treatment ($p>0.05$) compared to untreated cells (**Figure 11L**). 30 minutes after SKF treatment there was an increase in σ-1R colocalization with synaptophysin, however it was a statistically insignificant increase ($p>0.05$). 45 minutes

after SKF treatment the levels were similar to those of untreated cultures ($p>0.05$). The control pretreated with BD-1047 showed levels similar to untreated control cells ($p>0.05$).

These data suggest that σ-1R localizes somatically and extrasomatically in hippocampal slices when it is in its inactive state. With SKF treatment, IHC did not show a significant change in σ-1R at any subcellular compartment, although there was a mentionable increase in localization to dendrites and presynaptic terminals and decrease in σ-1R localization to PSDs. ICC also showed that σ-1R localizes to extrasynaptic regions. Also, there was a significant increase in σ-1R localization to dendrites after 30 minutes and PSDs after 15 minutes of treatment with SKF. Interestingly σ-1R colocalization with PSD-95, MAP-2, and synaptophysin decreases back to untreated levels after 45 minutes. The dendritic and PSD localization of σ-1R signifies that it localizes to the same subcellular compartments as NMDARs and PSD-95. Is it possible that σ-1R colocalization with NMDARs also increases after SKF treatment?

5.5. NMDAR Modulation by σ-1Rs

As previously mentioned, σ-1Rs were shown to modulate NMDARs (Figure 12)[14]. However, the mode of action for σ-1R modulation of NMDARs has not yet been determined. It has been questioned whether σ-1R modulation of NMDARs occurs through a direct interaction, or through a signaling method. Interestingly, work carried out by Mohan Pabba, a PhD candidate from our lab, has shown that the σ-1R forms a direct interaction with NMDARs and PSD-95 with and without activation (**Figure 13**). It is worth noting that more σ-1R protein can be co-IPed with GluN1, GluN2B, and PSD-95

after activation with SKF (**Figure 13A-B**). The reverse co-Ips have also been performed, and display the same results (**Figure 13C**).

In this study the relationship between σ-1Rs, NMDARs, and PSD-95 was assessed with ICA, in conjunction to percentage-based colocalization, to determine if the interaction might occur in neuronal projections. To test the modified ICA method, a HEK cell transfected with PSD-95-enhanced green fluorescent protein (eGFP), and co-labeled with PSD-95 antibody was assessed using the triple ICA technique I developed (**Figure 14**). As this image has two channels, the eGFP channel was used twice, as channel 1 and 3 (**Figure 4C**). The ICQ was found to be 0.26, and the percentage colocalization 53% (**Figure 14B**). This demonstrates dependent colocalization between the PSD-95 tagged eGFP and antibody, and indicates that the modified ICA method is functional.

σ-1R colocalization with PSD-95 and NMDARs was not measured in slices, as a good IHC antibody could not be found for GluN2A and GluN2B. Therefore these experiments were performed exclusively in dissociated neuron cultures. The 30-minute time point was selected for SKF treatment as it demonstrated the highest degree of colocalization for σ-1Rs and PSD-95.

Corresponding with co-IP data (**Figure 13**), σ-1Rs were found to colocalize with GluN2A and PSD-95 with and without SKF treatment (**Figure 15B-E**). There was no significant change in σ-1R colocalization with GluN2A and PSD-95 (**Figure 15D-E**).

σ-1Rs were also found to colocalize with PSD-95 and GluN2B with and without SKF treatment in cultures (**Figure 15G-J**). After a 30-minute treatment with SKF there was a statistically significant increase in σ-1R colocalization with GluN2B and PSD-95 that could be detected with the percentage-based method ($p<0.01$) of colocalization (**Figure**

15I). ICA detected the same level of dependent colocalization between σ-1Rs, GluN2B, and PSD-95 with and without SKF treatment (**Figure 15D,I**).

In summary, σ-1Rs colocalize with PSD-95 and GluN2A/2B with and without activation. However, after σ-1R activation there is a significant increase in colocalization with GluN2B and PSD-95.

6. Discussion

This study has demonstrated three main points corresponding with my initial hypotheses and aims. First, σ-1Rs localize extrasomatically without agonist treatment. Second, σ-1R localization increases in dendrites and PSDs in dissociated neuron cultures after treatment with agonist. Third, σ-1Rs colocalize with PSD-95 and NMDAR subunits GluN2A and GluN2B under untreated and SKF treated conditions *in vitro*. There is increased colocalization of σ-1R, PSD-95, and GluN2B upon treatment with σ-1R agonist.

6.1. σ-1R Localization

At the structural level, the distribution of σ-1Rs in the hippocampus (**Figure 7**) is similar to previous findings obtained with immunoperoxidase stain[19]. Notably, Alonso, et al. detected stronger localization of σ-1R to perikarya of dentate gyrus granule cells than we show here. As our antibody binds to the σ-1R C-terminus, which localizes to the ER lumen, it was not possible to obtain staining identical to that of the Alonso, et al. study without strong antigen retrieval. As our primary interest for this study was σ-1R localization in dendrites and colocalization with other antibodies, many of which were sensitive to strong antigen retrieval steps, this was not performed.

Here, we report for the first time detection of σ-1R subcellular localization in neurons through detection with immunofluorescence staining of IHC technique. Previous studies used radioligand binding and immunoperoxidase staining to identify σ-1R localization. The disadvantage to radioligand binding is that it does not allow for accurate protein localization studies, while disadvantages to immunoperoxidase localization include obscurement of the object being labeled, decreased accuracy in comparing protein

localization, and the presence of endogenous peroxidases. Furthermore, neither technique allows for colocalization analysis, limiting the ability for subcellular localization of σ-1Rs. Another concern with present σ-1R localization studies is the lack of agreement in the field resulting from inconsistencies in localization findings[19,20]. These discrepancies could stem from use of different model systems, protocols, or from problems with antibody specificity.

Based on previous immunofluorescence studies performed in heterologous systems it was expected that σ -1Rs would localize to perikarya. Also, as σ -1R modulates ion channels that reside in dendrites and PSDs it was expected that a subpopulation of σ -1Rs would also reside in dendrites and PSDs in close proximity to the ion channels it modulates. With the use of IHC in rat hippocampal slices and ICC in dissociated neuron cultures I demonstrated that σ-1Rs localize to dendrites and PSDs in untreated conditions (**Figure 8G-L, 11A-F**). Only male rats were used for slice preparations in order to avoid possible effects from endogenous pregnenolone sufate[31] or progesterone[32] in female rats. Localization of σ-1R to presynaptic terminals was minimal in untreated conditions, and might be attributable to noise (**Figure 8M-O, 11I-K**). This is consistent with previous findings that noted an absence of σ-1Rs presynaptically[19].

Interestingly, in dissociated cultures an accumulation of σ-1Rs was detected at dendritic branch points (**Figure 10B**), which has not been reported previously. This might correspond with the presence of complex ER networks at branch points, which confine mobility of membrane proteins[86]. These segments of increased ER complexity have been shown to preferentially express proteins involved in ER entry and exit within dendrites.

This restriction might have implications in the translocation of σ-1Rs to PSDs and extrasynaptic regions where it interacts with the ion channels it modulates.

6.2. Colocalization Analysis

Two methods of colocalization analysis were used in this study. The first is object-based colocalization, which assesses the degree of overlap between two channels. Object-based colocalization is ideal when quantifying colocalization for proteins that do not have a relationship[87]. It was therefore the only method of quantification used when analyzing σ-1R colocalization with cellular markers. The predominant disadvantage to this method is the inability to compare σ-1R localization between different cellular markers, as each cellular compartment can occupy a different volumes.

The second method used for colocalization analysis was a modified ICA, which allowed for analysis of colocalization between three channels simultaneously. The advantage to this technique is its ability to assess if colocalization obtained between proteins is random or dependent. It is ideal when studying interacting proteins[87], as they are expected to aggregate together in comparable amounts; therefore an assumption is made that the pixel intensity values can be used as an overall estimate of variation in quantity[75]. Also, as normalization is carried out relative to the number of pixels, this technique allows for comparison across different samples, and a discrete assessment of the relationship between multiple proteins. Notably, this is the first study to optimize ICA for detection of colocalization between three proteins. Effective quantification methods were not previously available for triple colocalization studies. For this reason and due to the inability of ICA to measure if colocalization is increasing or decreasing, percentage-

based colocalization was also performed when looking at colocalization between σ-1Rs, NMDAR subunits, and PSD-95.

6.3. σ -1R Activation in Slices

While previous studies have assessed σ -1R translocation after agonist treatment, all of these studies were performed in heterologous systems, which have limited similarities with neurons. Nonetheless, several studies have shown that σ -1Rs translocate towards the plasma membrane. Evidence for plasma membrane localization at this point is unconvincing, as both findings did not perform costaining, making it difficult to conclude if σ -1Rs are truly localizing at the plasma membrane[54,88]. Interestingly, Hayashi, et al. demonstrated that in NG-108 cells transfected with σ -1R-YFP, σ -1Rs move towards the tail of NG-108 cells. This suggests that the receptor might move towards dendrites in neurons[88].

Based on these findings for σ -1R translocation as well as its role in ion channel modulation, σ -1R up-regulation was expected in dendrites and PSDs after treatment with SKF. While our IHC data shows an increase in σ -1R localization to dendrites and presynaptic terminals, there was no statistical significance in the changes that were observed for σ -1R colocalization with MAP-2, PSD-95, and synaptophysin. The lack of change may have resulted selection of a time-point for SKF treatment that did not coincide with σ -1R translocation.

6.4. σ -1R Activation in Dissociated Cultures

Results obtained with dissociated neuron cultures showed σ -1R translocation to dendrites and PSDs after SKF activation. σ -1R proteins levels increased significantly in

PSDs after 15 minutes, and in dendrites after 30 minutes. Interestingly, there was a down-regulation of σ -1R localization with PSD-95 and MAP-2 45-minutes after initiation of SKF treatment. As the measured half-life for σ -1Rs is 72 hours[89], it is unlikely that the decrease in σ -1R levels is due to protein degradation. It is more likely that σ -1Rs are translocated out of the dendrites and PSDs, demonstrating the highly mobile nature of σ -1Rs.

While the colocalization of σ -1Rs with synaptophysin 30-minutes after SKF treatment displays large error bars, there is still a possibility that σ -1R translocates into presynaptic terminals after activation. In the future this will need to be investigated further by increasing sample sizes, and performing EM. σ-1R localization at presynaptic terminals after activation would not be surprising, as σ-1Rs display a variety of functions presynaptically[38,39,52,53,55-57]. The finding that σ -1R colocalization with PSD-95 increases after activation leads us to inquire if the activation of σ -1Rs would result in its colocalization with NMDARs. This is the first investigation of molecular mechanism behind σ -1R modulation of postsynaptic NMDARs.

6.5. σ -1R and NMDARs

It has been known for decades that σ-1Rs modulate NMDARs[7], however the molecular mechanism behind this relationship has not been established. While Martina, et al suggested that σ-1R potentiates NMDAR responses through SK-channel inhibition[67], without current-clamp electrophysiology recordings it is difficult to state with certainty that the inhibition of SK channels and the potentiation of NMDARs are interdependent events. Furthermore, co-IPs performed by Mohan Pabba, a PhD candidate from our lab, show that σ-1Rs, NMDARs, and PSD-95 form a complex. It should be taken into account

that while *in vitro* studies show a relationship between NMDARs and PSD-95[69,71], PSD-95 knockout animals do not display any changes in NMDAR surface expression[90]. It is possible that endogenously PSD-95 is only recruited as a scaffolding protein for NMDARs under certain circumstances, as PSD-95 knockout mice were only assessed at basal conditions, in which the σ-1R knockout mice also show no significant phenotype. I embarked on validating the association between σ-1Rs, NMDARs, and PSD-95 and identifying the site of this interaction with the use of immunofluorescence. I established that σ-1Rs colocalize dependently with NMDAR subunits and PSD-95 with SKF activation of σ-1Rs. I also found that σ-1Rs colocalize with PSD-95 and NMDAR subunits in the absence of σ-1R agonist. Based on previous findings that the σ-1R resides in the ER bound to BiP in its inactive state[24], this suggests that a subpopulation of σ-1Rs is active under basal conditions.

For σ-1R colocalization with GluN2A and PSD-95, the percentage of colocalization did not change (**Figure 15E**) although ICA showed a significant increase in dependent colocalization (**Figure 15D**). This suggests that although the three proteins reside in close proximity without σ-1R activation, σ-1R activation is required for them to dependently colocalize. Based on these findings it is more likely that σ-1R forms a complex with GluN2A and PSD-95 after activation with SKF. For σ-1R colocalization with PSD-95 and GluN2B there was a significant increase in the percentage of pixels that colocalized between the three proteins after σ -1R activation (**Figure 15J**). However the ICQs for σ-1R colocalization with PSD-95 and GluN2B did not change after treatment (**Figure 15I**). The consistency of ICQ values suggests that overall the colocalization obtained with and without treatment is dependent. Based on the significant increase in percentage-based

colocalization and the high ICQ associated with it, there seems to be an increase in association between σ-1Rs, GluN2B subunits, and PSD-95. It should be noted that the ability of ICA to measure complex formation is used here in conjunction with the co-IP findings (**Figure 13**), as ICA alone is not an effective measurement for complex formation[91].

6.6. Potential Implications of σ-1R Interaction with NMDARs

Learning the mechanism for σ -1R modulation of NMDARs has implications in improving the understanding of synaptic modifications. Also, it may help understand the neurological disorders that σ -1Rs have been linked to. Some of the disorders that σ -1Rs and/or NMDARs are linked to have been described below. As these are complex neurological diseases, which might have multiple pathways disrupted, the link between σ-1Rs and NMDARs is not the only solution to these disorders.

6.6.1. Amnesia and Alzheimer's Disease

Both cholinergic and glutamatergic systems are affected during aging, and have implications in amnesia[92]. In fact, a functional cooperation between cholinergic and glutamatergic systems might underlie the mechanism of learning and memory[93]. In amnesia models that function by the antagonism of NMDARs, administration of specific σ-1R agonist SA4503 resulted in improvement of the deficit in working and long-term memory[94]. However, σ-1R agonists have also been shown to have an effect on cholinergic neurotransmission[95]. It is therefore unknown if σ-1R agonists improve memory through the potentiation of NMDARs and cholinergic systems in a distinct mechanism, or if NMDAR-potentiation of cholinergic system underlies this effect. Alzheimer's disease is also characterized by cognitive and memory decline[96]. Genetic

polymorphisms of σ-1Rs have been shown to play a role in the severity of Alzheimer's disease[97]. The σ-1R agonist donezepil was shown to have neuroprotective effects[98], and it has been suggested that pre-administration of this drug could be used in the future to prevent Alzheimer's disease[97]. Analysis of postmortem human brains demonstrates a decrease in levels of σ-1Rs in the hippocampus of individuals with Alzheimer's disease[99].

6.6.2. Depression

Depression is characterized by a change in monoamine levels and NMDAR function[100]. The level of NMDAR subunit expression is decreased in depressed patients[101], and long-term use of NMDAR antagonists leads to symptoms of depression and anxiety[102]. Olfactory bulbectomized rats were used as a model of depression, as they display a dysfunctional glutamatergic system, on top of decreased monoamine levels[103]. When administered a σ-1R agonist, these rats show decreased symptoms of depression, increased levels of NMDAR subunit GluN1, and improved cognitive symptoms[104]. As NMDAR antagonist MK-801 abolishes the improvements achieved with σ-1R agonist, it can be concluded that σ-1R potentiation of NMDARs plays an important role in improving depressive and cognitive symptoms[104].

6.6.3. Amyotrophic Lateral Sclerosis (ALS)

ALS is characterized by a loss of motor neurons in the brain and spinal cord leading to muscle weakness and death from respiratory failure[105]. It was recently detected that a mutation in the σ-1R results in weaker cell resistance to apoptosis induced by ER stress, impacting ALS patients[106]. This corresponds with the motor deficiencies seen in σ-1R knockout mice[20].

6.7. Future Directions

The results for this study show for the first time that σ-1R levels are up-regulated in dendrites and PSDs after activation. As this occurs in a relatively short time period, it might be assumed that σ-1Rs translocate from the cell body. In the future, live imaging could help confirm this.

This is also the first time that σ-1R colocalization was measured relative to NMDARs. The fact that there is an increase in colocalization of σ-1R with NMDAR subunits and PSD-95 after σ-1R activation suggests that σ-1R translocation is an important aspect in σ-1R potentiation of NMDARs. However, many more questions still remain with regards to the mechanism behind σ-1R modulation of NMDARs. First, based on the immunofluorescence alone it cannot be concluded that a direct interaction occurs. Furthermore, it is not known if PSD-95 is essential in the interaction between NMDARs and σ-1Rs. Another question that remains is if NMDARs are potentiated through up-regulation at the plasma membrane or through gating mechanisms. Whether or not translocation of σ -1R to dendrites and PSDs is important to voltage-gated ion channels should also be investigated in future studies.

7. Conclusion

This study has demonstrated that σ -1Rs localize to dendrites and PSDs. Furthermore I have shown that σ -1R localization at PSDs and dendrites increases after activation. Lastly, colocalization was detected between the σ-1R, NMDAR, and PSD-95 with and without σ -1R activation. This supports the presence of a direct interaction between σ-1Rs and NMDARs in the modulation of the glutamate-gated ion channel. This may suggest a possible mechanism behind σ-1R regulation of voltage-gated ion channels.

8. Tables

Compound	Subtype Selectivity	K_i or K_D for σ-1R Site	Function on σ-1R Site
Benzomorphans			
(+)-Pentazocine	σ-1	+++	Agonist
(–)-Pentazocine	σ-1/σ-2	++	Agonist
(+)-SKF-10,047	σ-1	+++	Agonist
Antipsychotics			
Chlorpromazine	σ-1/σ-2	++	Unknown
Haloperidol	σ-1/σ-2	+++	Antagonist
Nemonapride	σ-1/σ-2?	+++	Unknown
Antidepressants			
Clorgyline	σ-1	+++	Agonist?
Fluoxetine	σ-1	+	Agonist
Fluvoxamine	σ-1	+++	Agonist
Imipramine	σ-1	++	Agonist
Sertraline	σ-1	++	Agonist
Antitussives			
Dextromethorphan	σ--1	++	Agonist
Putative Endogenous Ligands (Neurosteroids)			
DHEAS	σ-1	+	Agonist
Pregnenolone sulfate	σ-1	+	Agonist
Progesterone	σ-1	+	Antagonist
Anticonvulsants			
Phenytoin (DPH)	σ-1	Not applicable	Allosteric Modulator
Ropizine	σ-1	Not applicable	Allosteric modulator
Other σ drugs			
BD 737	σ-1/σ2	+++	Agonist
BD 1008	σ-1/σ2	+++	Antagonist
BD 1047	σ-1	+++	Antagonist
BD 1063	σ-1	+++	Antagonist
DTG	σ-1/σ2	+++	Unknown
Eliprodil	σ-1/σ2	++	Unknown
JO-1784 (Igmesine)	σ-1	+++	Agonist
Metaphit	σ-1/σ2	++	Antagonist
NE-100	σ-1	+++	Antagonist
(+)-3-PPP	σ-1/σ2	++	Agonist
PRE 084	σ-1	+++	Agonist
Rimcazole	σ-1/σ2	+	Antagonist
SA4503	σ-1	+++	Agonist
SR 31742A	Unknown	+++	Unknown

Table 1. Common σ-1R ligands. The most common ligands utilized for the σ-1R, with the specificity for the σ-1 versus σ-2 receptor, level of affinity for the σ-1R, and function on the σ-1R. The affinities: + refers to an affinity of less than 10μM, ++ refers to less than 500nM, and +++ refers to less than 50nm. This table is a modification of one shown by Cobos, et al[107].

Antibody	Species	Concentration	Company
Primary Antibodies			
GFAP	Chicken	1:2500*	EnCor Biotech
NeuN	Mouse	1:300*; 1:600**	Millipore
GluN1	Mouse	1:1000*; 1:8000**	Synaptic Systems
GluN2A	Mouse	1:1000**	LifeSpan
GluN2B	Mouse	1:1000**	LifeSpan
PSD-95	Goat	1:250*, 1:500**	Abcam
MAP-2	Chicken	1:5000*; 1:20000**	EnCor Biotech
σ-1R (by Su)	Rabbit	1:500*	Gift from Dr. Su
σ-1R	Rabbit	1:200***	Abcam
Synaptophysin	Mouse	1:2000*; 1:5000*	Sigma
Secondary Antibodies			
Alexa-647	Donkey Anti-Rabbit (DARb)	1:200***	Jackson Immunoresearch
CY5	Donkey Anti-Mouse (DAM)	1:200***	Jackson Immunoresearch
CY3	Goat Anti-Chicken (GACk)	1:200***	Jackson Immunoresearch
FITC	Donkey Anti-Goat (DAG)	1:100*, 1:200**	JacksonImmunoresearch

Table 2. List of antibodies used. Table includes the species antibodies were raised in, company purchased from, and concentration used. * indicates a concentration used in slices, while ** indicates a concentration used in hippocampal cultures, *** is used when a concentration is optimal for both slices and cultures.

9. Figures

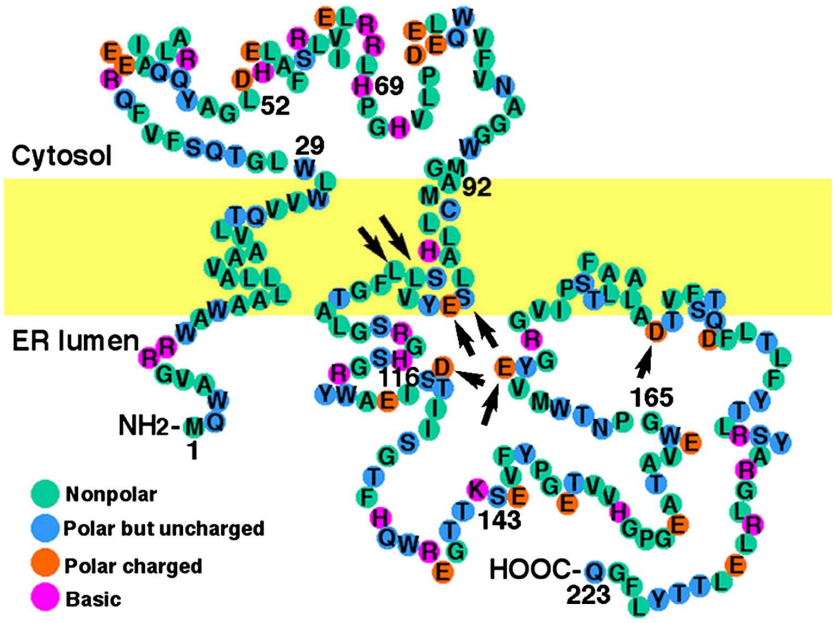

Figure 1. The proposed structure of the σ-1R. The σ-1R consists of 223 amino acids, two transmembrane domains, and three hydrophobic domains. The N- and C-termini localize to the ER lumen, and in oocytes were shown to enter the plasma membrane with the N- and C-termini facing the cytosol. The ligand-binding sites, which are contained within the C-terminus and second hydrophobic domain sites are indicated with arrows. This image was acquired from a paper by Hayashi and Su[24].

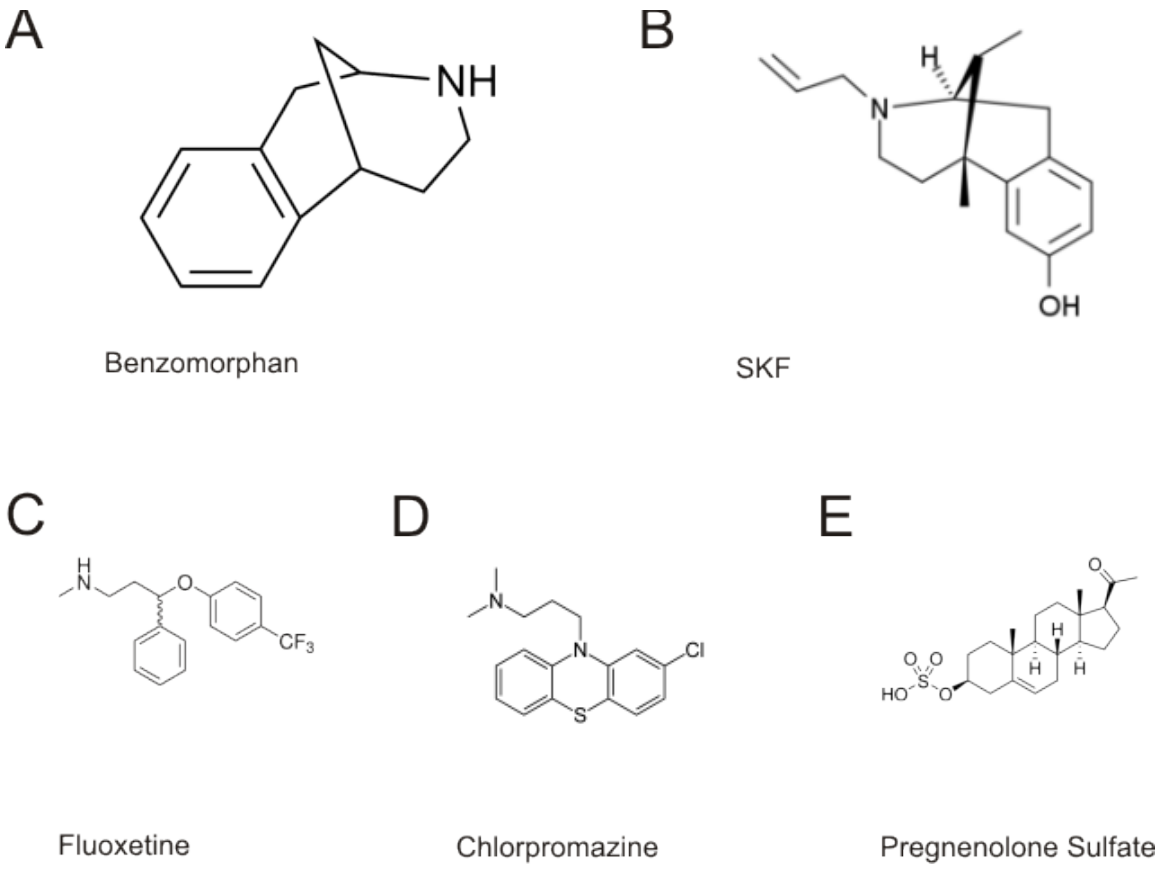

Figure 2. Benzomorphan structure. (A) The benzomorphan skeleton is a common feature among the σ-1R ligands. (B) It is also the base for many σ-1R ligands that were synthetically developed, such as SKF. Some common σ-1R ligands include SSRIs (C) fluoxetine, clorgyline, and sertraline; antipsychotics (D) chlorpromazine and haloperidol; and neurosteroids (E) pregnenolone sulfate, DHEA, and progesterone.
[Online] URL: http://en.wikipedia.org/wiki/Benzomorphan; http://www.evi.com/q/facts_about__alazocine_2; http://en.wikipedia.org/wiki/Fluoxetine; http://en.wikipedia.org/wiki/Chlorpromazine; http://en.wikipedia.org/wiki/Pregnenolone

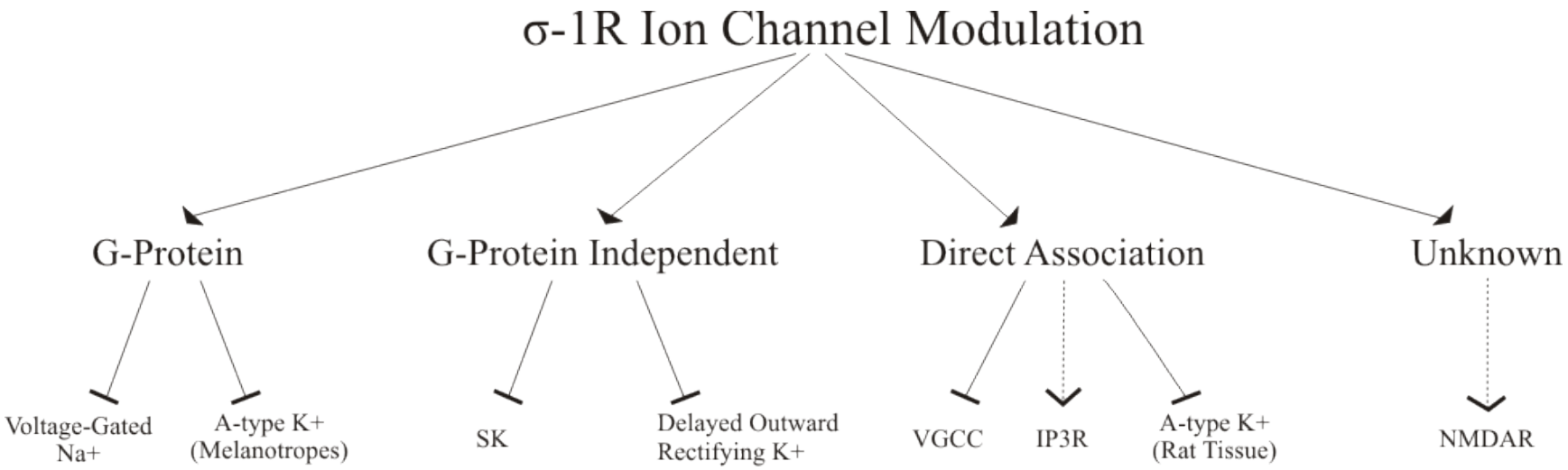

Figure 3. Schematic representation of ion channels modulated by the σ-1R. The σ-1R has been shown to inhibit voltage-gated ion channels and potentiate ligand-gated ion channels. σ-1Rs modulate the following voltage-gated ion channels: Na^+ channels, A-type K^+ channels, SK channels, and delayed outward rectifying K^+ channels. While it is known that σ-1Rs modulate the ligand-gated IP3Rs through a direct interaction, it is not known how NMDARs are modulated by the σ-1R. Dotted arrows represent ion channels that are potentiated, and a solid line with blunt end indicates ion channels inhibited by the σ-1R. Information for this figure was acquired from the following references: 16,19, 45-49, 51.

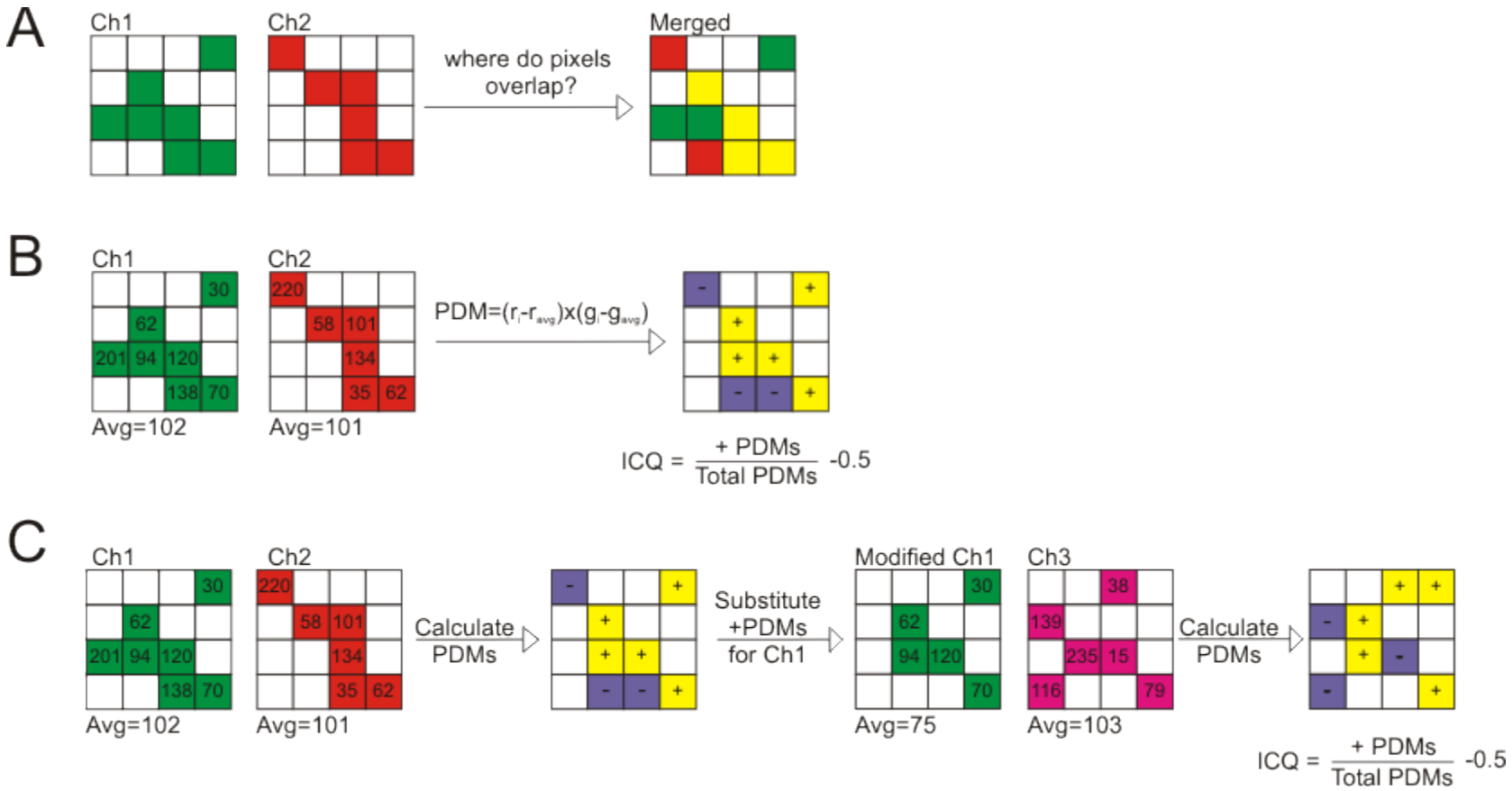

Figure 4. Schematic of object-based and ICA quantification for colocalization analysis. (A) Channel (Ch) 1 (green) and 2 (red) are represented as pixels. Overlapped pixels (yellow) are measured as a percentage of total pixels in Ch1 and Ch2. (B) ICA utilizing two channels requires knowledge of pixel intensity values and channel averages. Positive PDMs (dependent colocalization) are represented with yellow pixels and negative PDMs (independent colocalization) with purple. An ICQ is calculated based on the above formula, which is an indication of the overall dependence or randomness in colocalization. (C) ICA utilizing three channels was performed by first calculating PDMs with Ch1 and Ch2. A modified Ch1 is created where only pixels that dependently colocalize (PDM>0) with Ch2 are included. The modified Ch1 and Ch3 are then analyzed in the same manner as regular ICA (B).

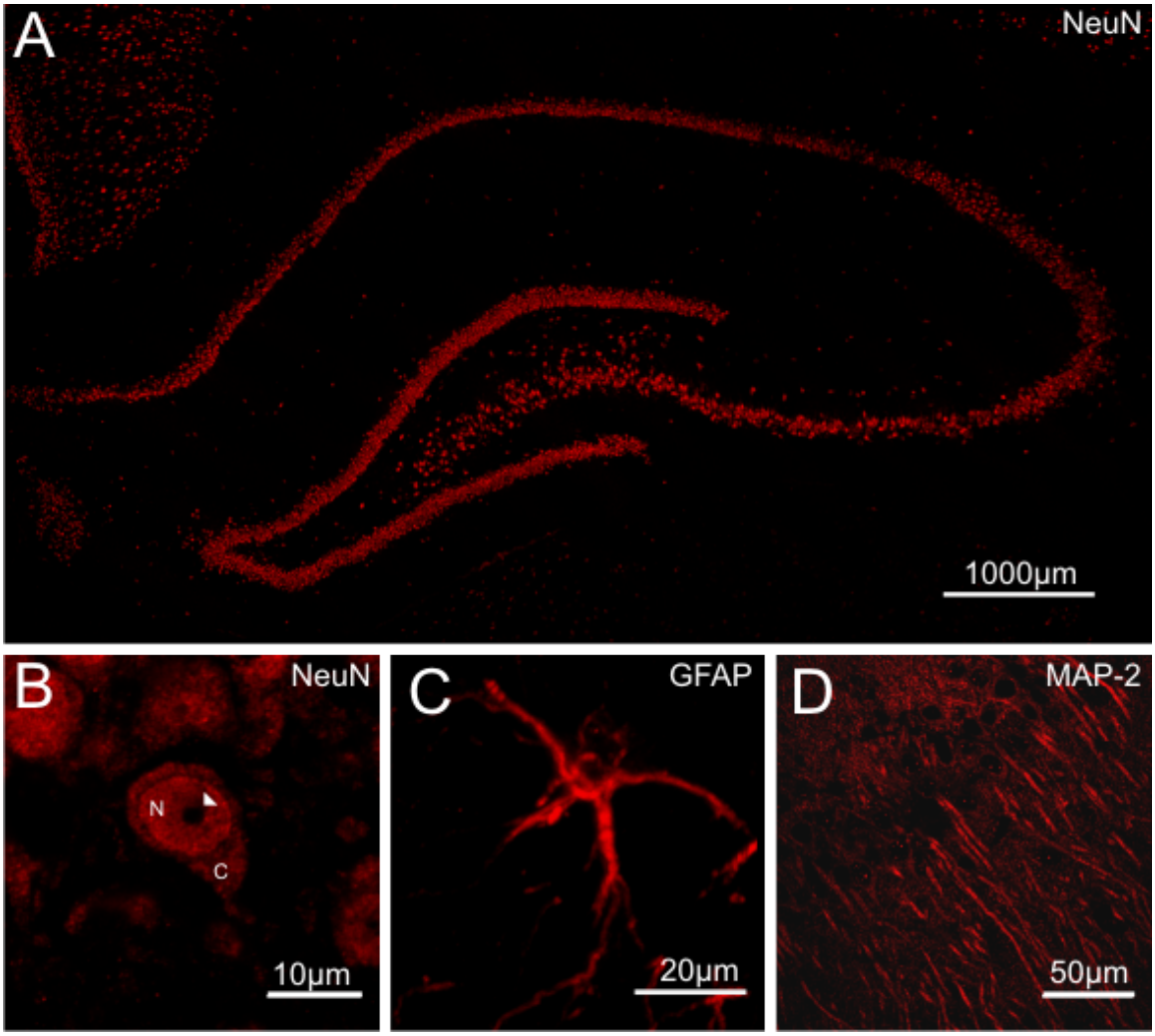

Figure 5. Characterization of neurons and glia in the hippocampus. Hippocampal slices were immunofluorescently stained with NeuN to label cell bodies at a (A) low (70x) and (B) high magnification (2520x). Immunofluorescent labeling was also performed for (C) GFAP (2520x), and (D) MAP-2 (441x). "N" signifies the nucleus, "C" the cytoplasm, arrowhead points towards the unstained region in the nucleus.

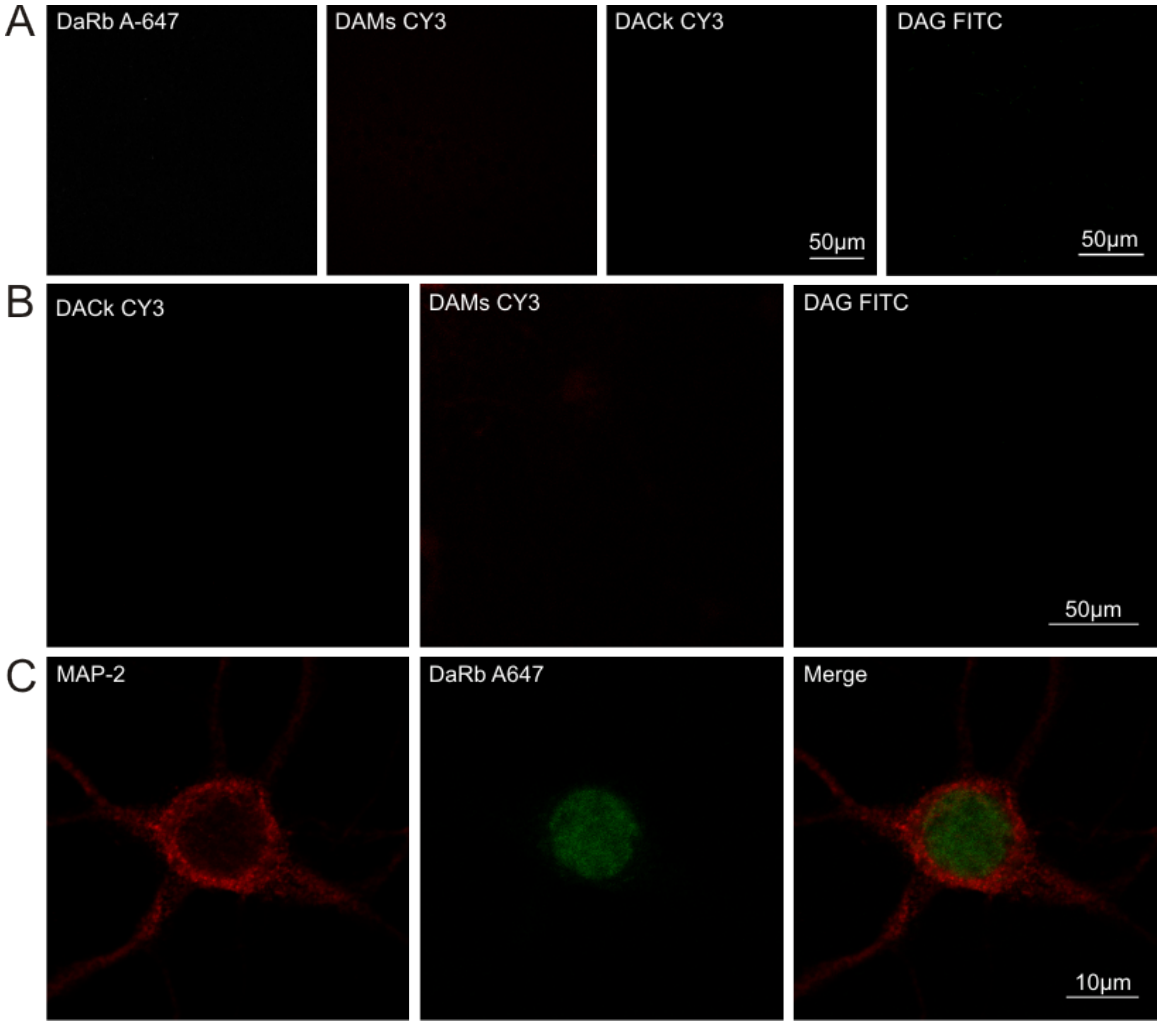

Figure 6. Controls omitting primary antibody. (A) Hippocampal slices immunofluorescently labeled with secondary antibodies Donkey Anti-Rabbit (DARb) Alexa-647 (A647), Donkey Anti-Mouse (DAM) CY3, Donkey Anti-Chicken (DACk) CY3, and Donkey Anti-Goat (DAG) FITC. (B) Dissociated neurons labeled in the absence of primary antibody with DACk CY3, DAMs CY3, and DAG FITC. (C) Dissociated neuron cultures co-labeled with DARb Alexa-647 (green) secondary antibody and MAP-2 (red), with the merged image shown.

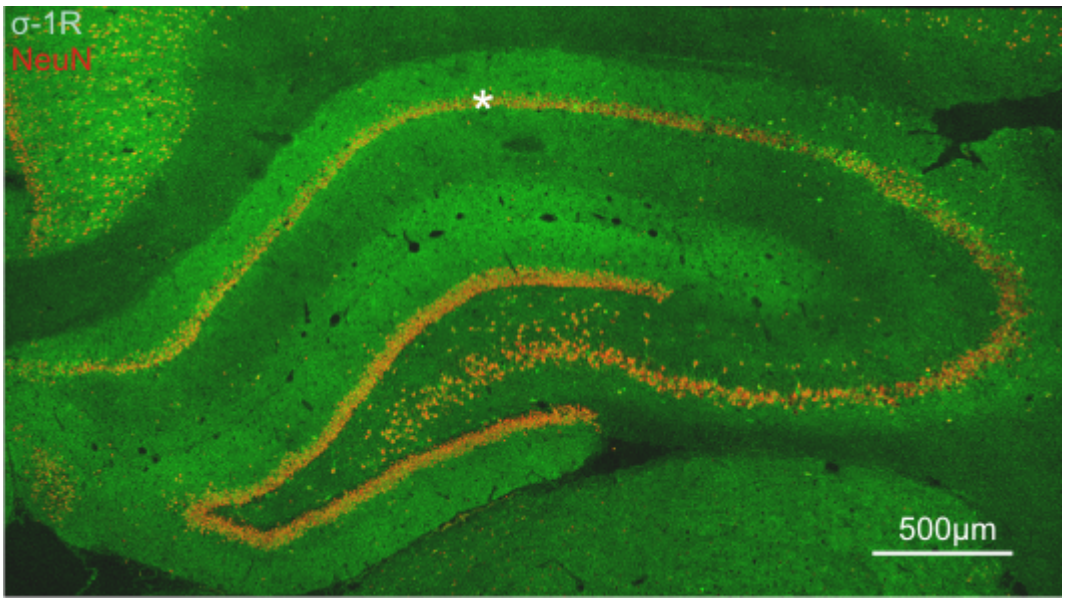

Figure 7. σ-1Rs predominantly localize to cell bodies and the stratum moleculare in the hippocampus. σ-1Rs (green) were co-stained with NeuN (red) in hippocampal slices. An asterisk indicates where high magnification images were taken for colocalization analysis.

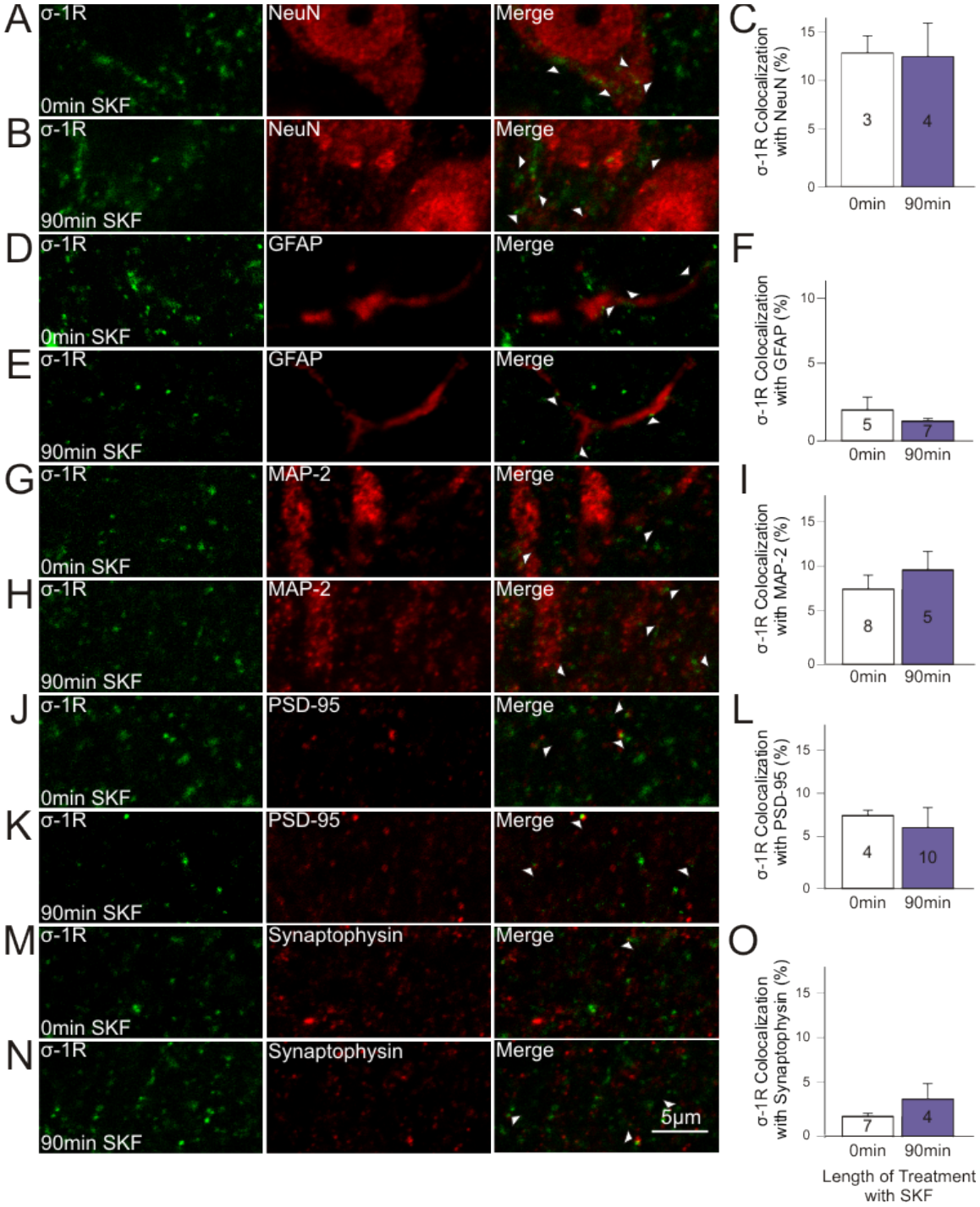

Figure 8. σ-1R localization in hippocampal slices does not change after activation with SKF. High magnification (2520x) images of hippocampal slices from 90-minute (min) SKF treated and untreated male rats were immunofluorescently labeled with σ-1Rs (green) and various cellular markers (red). σ-1Rs and NeuN were co-labeled in the absence (A) and presence (B) of σ-1R activation. (C) Quantitative colocalization analysis was plotted. σ-1Rs and GFAP were co-labeled without (D) and with (E) activation of σ-1Rs. (F) Quantitative colocalization analysis was plotted. σ-1Rs and MAP-2 were co-

labeled without (G) and with (H) activation of σ-1Rs. (I) Quantitative colocalization analysis was plotted. σ-1Rs and PSD-95 were co-labeled without (J) and with (K) activation of σ-1Rs. (L) Quantitative colocalization analysis was plotted. σ-1Rs and synaptophysin were co-labeled without (M) and with (N) activation of σ-1Rs. (O) Quantitative colocalization analysis was plotted. Arrowheads depict colocalized pixels. Numbers plotted in columns indicate the number of cells assessed in at least two animals. Values are averages ± SEM.

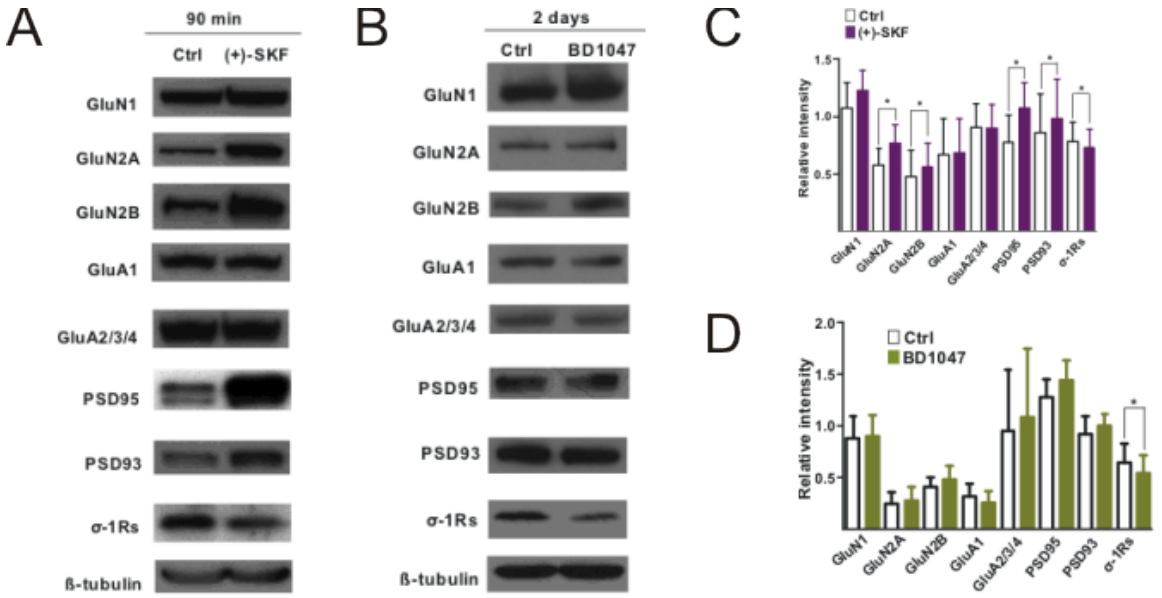

Figure 9. NMDAR and PSD-95 levels increase in hippocampal synaptosomal fractions after SKF treatment. (A) Rats were treated with SKF for 90 minutes, and Western Blots performed on synaptosomal membranes isolated from the hippocampus. (C) Relative intensity quantification of the bands was plotted. (B) Controls were performed by pretreating rats with BD-1047 for 2 days prior to SKF treatment. (D) Relative intensity quantification was plotted.
Figure of unpublished results obtained from Mohan Pabba.

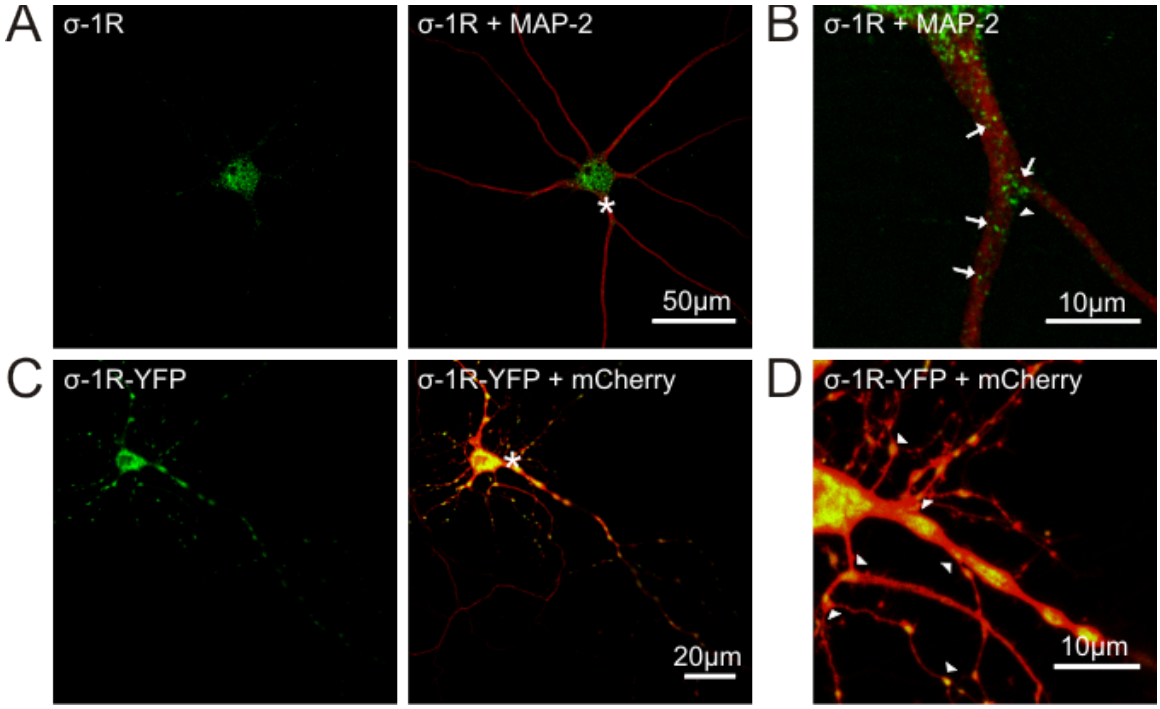

Figure 10. σ-1Rs localize extrasomatically, with an apparent preference towards dendritic branch points. σ-1Rs (green) were immunofluorescently colabelled with MAP-2 (red) in banker cultures as shown with low (441x) and high (2520x) magnification images. High density dissociated neuron cultures were transfected with σ-1R-YFP (green) and mCherry (red), and depicted with low (400x) and high (2400x) magnification images. Arrowheads represent localization of σ-1Rs at branch points, and arrows represent colocalization of σ-1R with MAP-2.

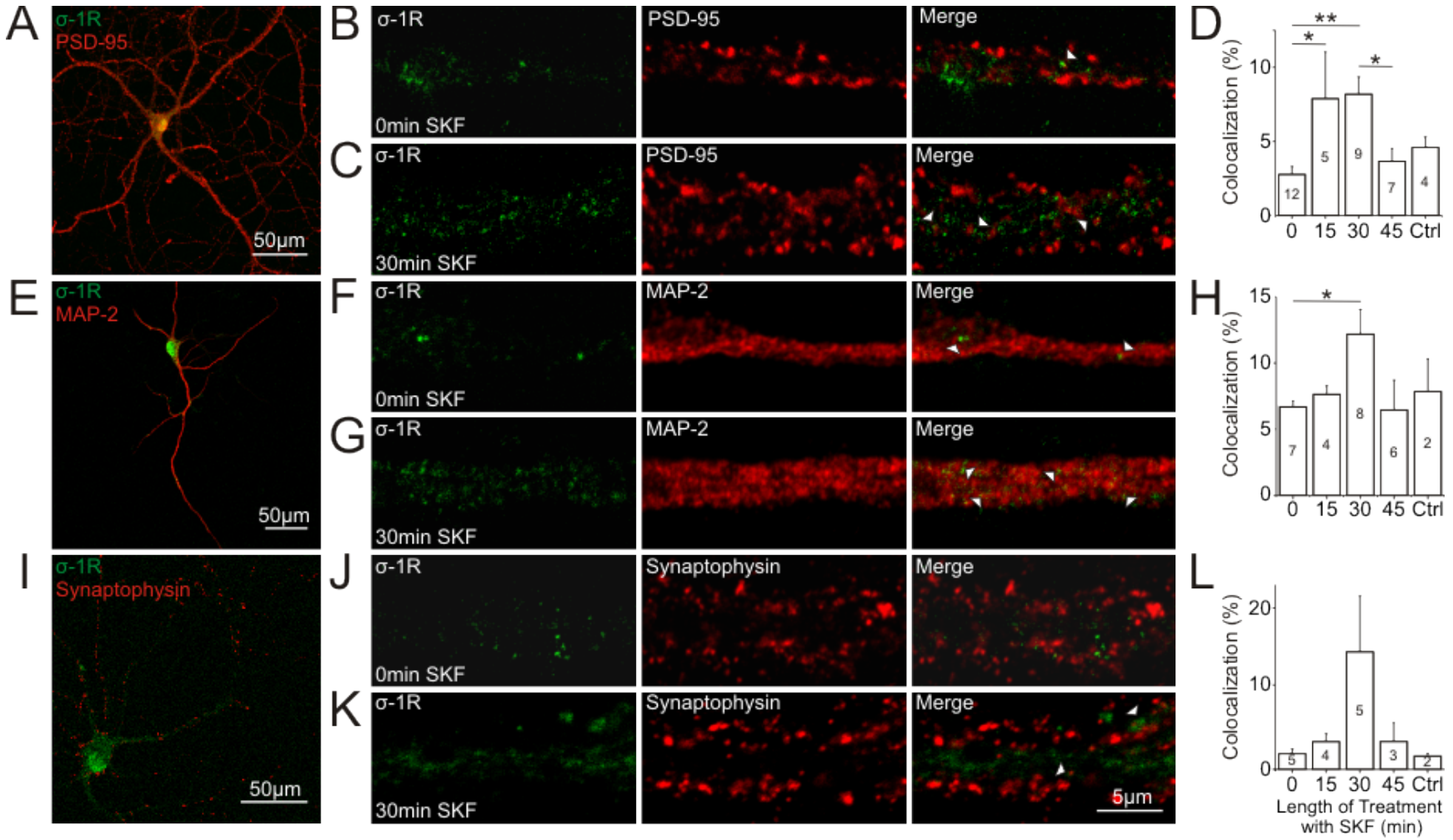

Figure 11. In dissociated neuron cultures σ-1R localization at dendrites and PSDs increases after treatment with SKF. Dissociated neuron cultures were labeled with σ-1R (green) and extrasomatic cellular markers (red) (A) PSD-95, (E) MAP-2, and (I) synaptophysin. Controls (Ctrls) were performed with BD-1047 pretreatment for two hours, followed by 30-min SKF treatment. High

magnification (2520x) images were taken for colocalization analysis. σ-1Rs were co-labeled with PSD-95 in the absence (B) and presence (C) of SKF treatment. (D) Quantification of colocalization was plotted for the various time points at which the experiment was performed. σ-1Rs were co-labeled with MAP-2 in the absence (F) and presence (G) of SKF treatment. (H) Quantification of colocalization was plotted for the various time points at which the experiment was performed. σ-1Rs were co-labeled with PSD-95 in the absence (J) and presence (K) of SKF treatment. (L) Quantification of colocalization was plotted for the various time points at which the experiment was performed. Arrowheads point out colocalization between σ-1Rs and cellular markers. Numbers plotted in columns indicated the number of cells assessed in at least 3 experiments. Values are averages ± SEM.

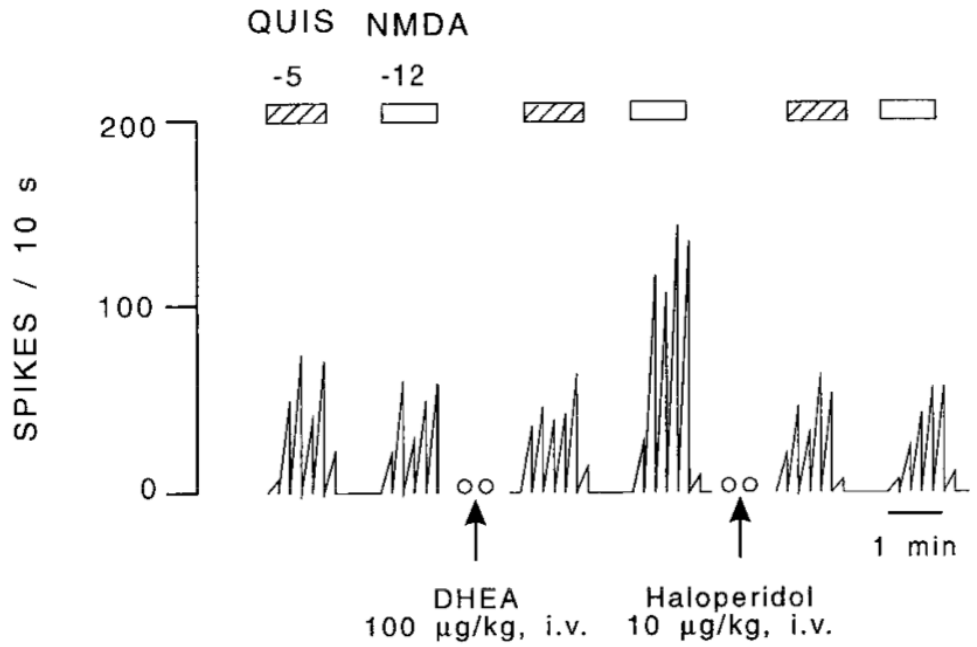

Figure 12. NMDAR firing frequency is potentiated by the σ-1R. Rats were mounted in a stereotaxic apparatus. NMDAR and α-amino-3-hydroxy-5-methyl-4-isoxazolepropionic acid receptor (AMPAR) agonists quisqualate (QUIS) and *N*-methyl-D-aspartate (NMDA) were applied microiontophoretically before and after intravenous injection with σ-1R agonist DHEA in the CA3. The firing frequency was measured using extracellular unitary recordings. As a control animals were injected with σ-1R antagonist haloperidol. This image was acquired from a paper by Bergeron et al[30].

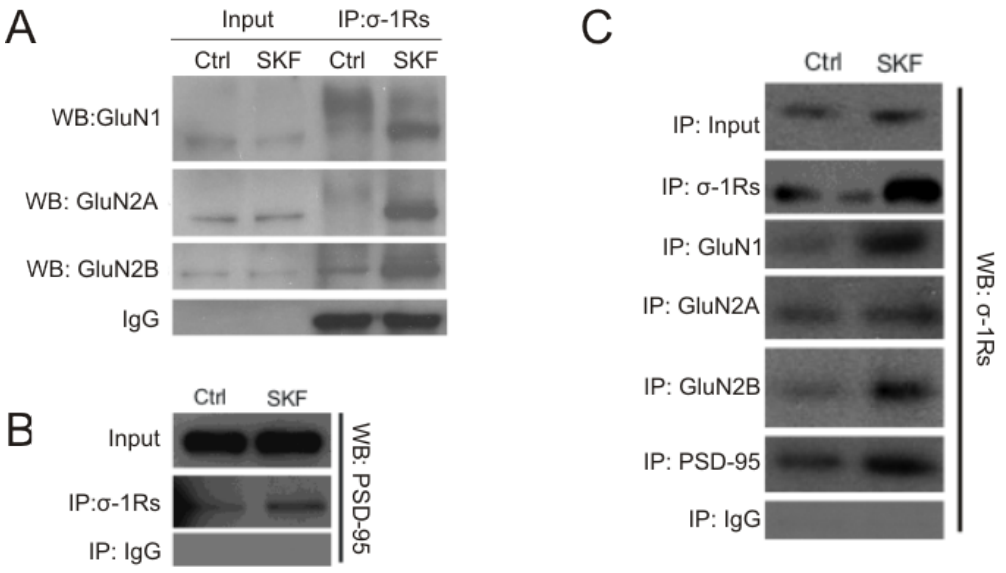

Figure 13. σ-1Rs form a complex with NMDARs and PSD-95. Rats were treated with 1mg/kg SKF for 90 mins through an intraperitoneal injection. Control animals were given saline injections. Co-IPs were performed with rat hippocampi by Mohan Pabba, a PhD candidate from Richard Bergeron's lab. (A) NMDARs and (B) PSD-95 were pulled down through a σ-1R co-IP. (C) A reverse co-IP with NMDARs and PSD-95 showed pull-down of σ-1Rs.
Figure of unpublished results obtained from Mohan Pabba.

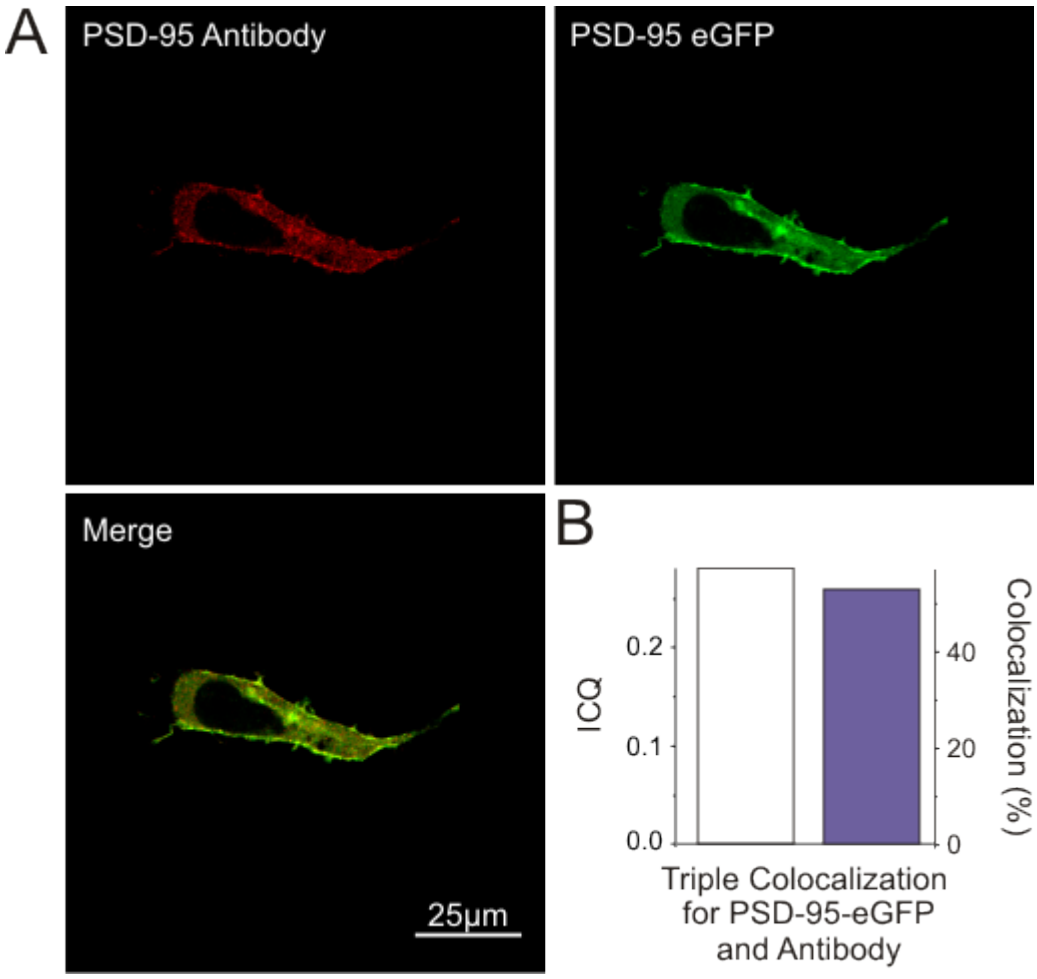

Figure 14. PSD-95-eGFP co-labelling with PSD-95 antibody was used as a positive control for ICA. (A) HEK cells transfected with PSD-95-eGFP were immunofluorescently colabelled with PSD-95 antibody (red) (B) Triple colocalization was calculated with the percentage-based and ICA methods by using the PSD-95-eGFP channel twice.

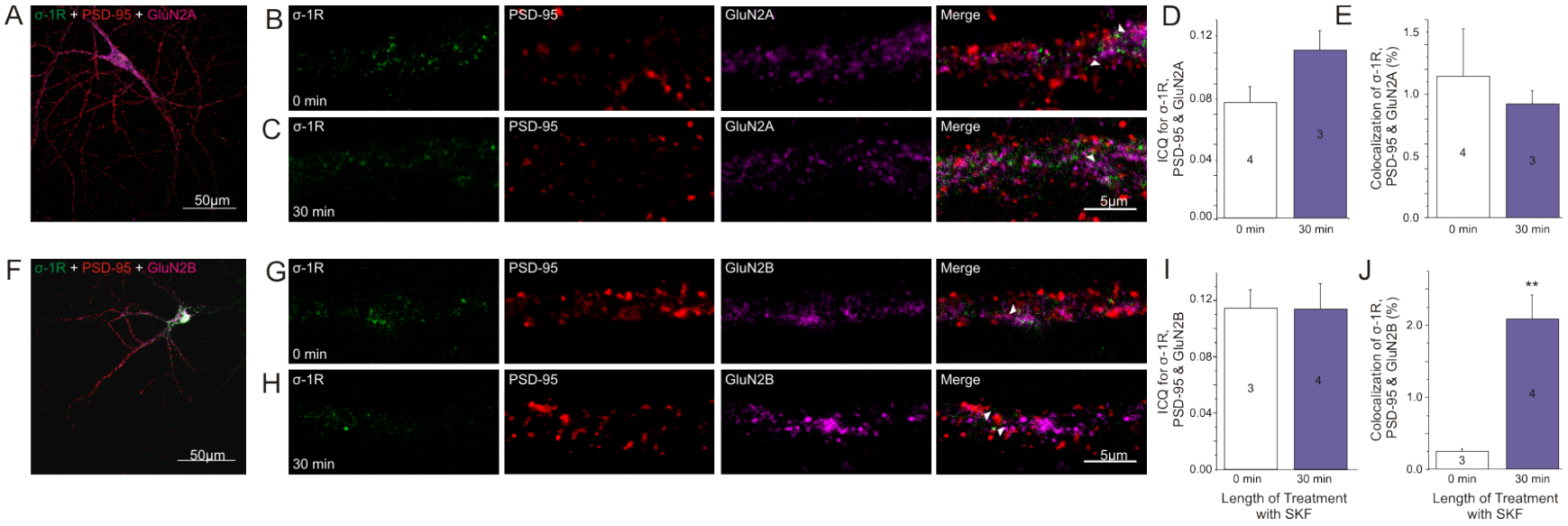

Figure 15. There is increased colocalization between σ-1R, GluN2B, and PSD-95 after SKF activation, and increased dependent association between σ-1R, GluN2A, and PSD-95. Dissociated neuron cultures were costained with σ-1R, PSD-95, and NMDAR subunits (A) GluN2A or (F) GluN2B (630x). High magnification images were taken for colocalization analysis (2520x). Colocalization was assessed between σ-1R, GluN2A, and PSD-95 (B) without and (C) with SKF. Colocalization was quantified with percentage-based colocalization (D) and ICA (E). Colocalization was assessed for σ-1R, GluN2B, and PSD-95 (G) without and (H) with SKF. Colocalization was quantified with percentage-based colocalization (I) and ICA (J). Arrowheads indicate colocalization between σ-1Rs, PSD-95, and NMDAR subunits. Numbers plotted in columns indicated sample size. Values are averages ± SEM.

10. References

1 Levitan, I. B. Modulation of ion channels in neurons and other cells. *Annual review of neuroscience* **11**, 119-136, doi:10.1146/annurev.ne.11.030188.001003 (1988).

2 Waxman, S. G. The neuron as a dynamic electrogenic machine: modulation of sodium-channel expression as a basis for functional plasticity in neurons. *Philosophical transactions of the Royal Society of London. Series B, Biological sciences* **355**, 199-213, doi:10.1098/rstb.2000.0559 (2000).

3 Hayashi, T. & Su, T. The sigma receptor: evolution of the concept in neuropsychopharmacology. *Current neuropharmacology* **3**, 267-280 (2005).

4 Li, Z. *et al.* Dehydroepiandrosterone sulfate prevents ischemia-induced impairment of long-term potentiation in rat hippocampal CA1 by up-regulating tyrosine phosphorylation of NMDA receptor. *Neuropharmacology* **51**, 958-966, doi:10.1016/j.neuropharm.2006.06.007 (2006).

5 Maurice, T., Phan, V. L. & Privat, A. The anti-amnesic effects of sigma1 (sigma1) receptor agonists confirmed by in vivo antisense strategy in the mouse. *Brain research* **898**, 113-121 (2001).

6 Zhang, H., Katnik, C. & Cuevas, J. Sigma receptor activation inhibits voltage-gated sodium channels in rat intracardiac ganglion neurons. *International journal of physiology, pathophysiology and pharmacology* **2**, 1-11 (2009).

7 Bergeron, R., Debonnel, G. & De Montigny, C. Modification of the N-methyl-D-aspartate response by antidepressant sigma receptor ligands. *European journal of pharmacology* **240**, 319-323 (1993).

8 Regehr, W. G. & Tank, D. W. Postsynaptic NMDA receptor-mediated calcium accumulation in hippocampal CA1 pyramidal cell dendrites. *Nature* **345**, 807-810, doi:10.1038/345807a0 (1990).

9 Gilbert, P. E. & Martin, W. R. Sigma effects of nalorphine in the chronic spinal dog. *Drug and alcohol dependence* **1**, 373-376 (1976).

10 Su, T. P. Evidence for sigma opioid receptor: binding of [3H]SKF-10047 to etorphine-inaccessible sites in guinea-pig brain. *The Journal of pharmacology and experimental therapeutics* **223**, 284-290 (1982).

11 Hellewell, S. B. *et al.* Rat liver and kidney contain high densities of sigma 1 and sigma 2 receptors: characterization by ligand binding and photoaffinity labeling. *European journal of pharmacology* **268**, 9-18 (1994).

12 Hanner, M. *et al.* Purification, molecular cloning, and expression of the mammalian sigma1-binding site. *Proceedings of the National Academy of Sciences of the United States of America* **93**, 8072-8077 (1996).

13 Seth, P., Leibach, F. H. & Ganapathy, V. Cloning and structural analysis of the cDNA and the gene encoding the murine type 1 sigma receptor. *Biochemical and biophysical research communications* **241**, 535-540, doi:10.1006/bbrc.1997.7840 (1997).

14 Prasad, P. D. *et al.* Exon-intron structure, analysis of promoter region, and chromosomal localization of the human type 1 sigma receptor gene. *Journal of neurochemistry* **70**, 443-451 (1998).
15 Seth, P. *et al.* Cloning and functional characterization of a sigma receptor from rat brain. *Journal of neurochemistry* **70**, 922-931 (1998).
16 Aydar, E., Palmer, C. P., Klyachko, V. A. & Jackson, M. B. The sigma receptor as a ligand-regulated auxiliary potassium channel subunit. *Neuron* **34**, 399-410 (2002).
17 Chen, Y., Hajipour, A. R., Sievert, M. K., Arbabian, M. & Ruoho, A. E. Characterization of the cocaine binding site on the sigma-1 receptor. *Biochemistry* **46**, 3532-3542, doi:10.1021/bi061727o (2007).
18 Pal, A. *et al.* Identification of regions of the sigma-1 receptor ligand binding site using a novel photoprobe. *Molecular pharmacology* **72**, 921-933, doi:10.1124/mol.107.038307 (2007).
19 Alonso, G. *et al.* Immunocytochemical localization of the sigma(1) receptor in the adult rat central nervous system. *Neuroscience* **97**, 155-170 (2000).
20 Mavlyutov, T. A., Epstein, M. L., Andersen, K. A., Ziskind-Conhaim, L. & Ruoho, A. E. The sigma-1 receptor is enriched in postsynaptic sites of C-terminals in mouse motoneurons. An anatomical and behavioral study. *Neuroscience* **167**, 247-255, doi:10.1016/j.neuroscience.2010.02.022 (2010).
21 Hayashi, T. & Su, T. P. Sigma-1 receptors at galactosylceramide-enriched lipid microdomains regulate oligodendrocyte differentiation. *Proceedings of the National Academy of Sciences of the United States of America* **101**, 14949-14954, doi:10.1073/pnas.0402890101 (2004).
22 Palacios, G. *et al.* Immunohistochemical localization of the sigma1-receptor in oligodendrocytes in the rat central nervous system. *Brain research* **961**, 92-99 (2003).
23 Palacios, G., Muro, A., Verdu, E., Pumarola, M. & Vela, J. M. Immunohistochemical localization of the sigma1 receptor in Schwann cells of rat sciatic nerve. *Brain research* **1007**, 65-70, doi:10.1016/j.brainres.2004.02.013 (2004).
24 Hayashi, T. & Su, T. P. Sigma-1 receptor chaperones at the ER-mitochondrion interface regulate Ca(2+) signaling and cell survival. *Cell* **131**, 596-610, doi:10.1016/j.cell.2007.08.036 (2007).
25 Koe, B. K., Burkhart, C. A. & Lebel, L. A. (+)-[3H]3-(3-hydroxyphenyl)-N-(1-propyl)-piperidine binding to sigma receptors in mouse brain in vivo. *European journal of pharmacology* **161**, 263-266 (1989).
26 Largent, B. L., Wikstrom, H., Gundlach, A. L. & Snyder, S. H. Structural determinants of sigma receptor affinity. *Molecular pharmacology* **32**, 772-784 (1987).
27 Zamanillo, D. *et al.* Up-regulation of sigma(1) receptor mRNA in rat brain by a putative atypical antipsychotic and sigma receptor ligand. *Neuroscience letters* **282**, 169-172 (2000).
28 Hashimoto, K. Sigma-1 receptors and selective serotonin reuptake inhibitors: clinical implications of their relationship. *Central nervous system agents in medicinal chemistry* **9**, 197-204 (2009).

29 Su, T. P., London, E. D. & Jaffe, J. H. Steroid binding at sigma receptors suggests a link between endocrine, nervous, and immune systems. *Science* **240**, 219-221 (1988).
30 Bergeron, R., de Montigny, C. & Debonnel, G. Potentiation of neuronal NMDA response induced by dehydroepiandrosterone and its suppression by progesterone: effects mediated via sigma receptors. *The Journal of neuroscience : the official journal of the Society for Neuroscience* **16**, 1193-1202 (1996).
31 Flood, J. F., Morley, J. E. & Roberts, E. Pregnenolone sulfate enhances post-training memory processes when injected in very low doses into limbic system structures: the amygdala is by far the most sensitive. *Proceedings of the National Academy of Sciences of the United States of America* **92**, 10806-10810 (1995).
32 Urani, A., Privat, A. & Maurice, T. The modulation by neurosteroids of the scopolamine-induced learning impairment in mice involves an interaction with sigma1 (sigma1) receptors. *Brain research* **799**, 64-77 (1998).
33 Maurice, T., Urani, A., Phan, V. L. & Romieu, P. The interaction between neuroactive steroids and the sigma1 receptor function: behavioral consequences and therapeutic opportunities. *Brain research. Brain research reviews* **37**, 116-132 (2001).
34 Langa, F. *et al.* Generation and phenotypic analysis of sigma receptor type I (sigma 1) knockout mice. *The European journal of neuroscience* **18**, 2188-2196 (2003).
35 Chevallier, N., Keller, E. & Maurice, T. Behavioural phenotyping of knockout mice for the sigma-1 (sigma(1)) chaperone protein revealed gender-related anxiety, depressive-like and memory alterations. *J Psychopharmacol* **25**, 960-975, doi:10.1177/0269881111400648 (2011).
36 Aydar, E., Onganer, P., Perrett, R., Djamgoz, M. B. & Palmer, C. P. The expression and functional characterization of sigma (sigma) 1 receptors in breast cancer cell lines. *Cancer letters* **242**, 245-257, doi:10.1016/j.canlet.2005.11.011 (2006).
37 Tsai, S. Y. *et al.* Sigma-1 receptors regulate hippocampal dendritic spine formation via a free radical-sensitive mechanism involving Rac1xGTP pathway. *Proceedings of the National Academy of Sciences of the United States of America* **106**, 22468-22473, doi:10.1073/pnas.0909089106 (2009).
38 Lu, C. W., Lin, T. Y., Wang, C. C. & Wang, S. J. sigma-1 Receptor agonist SKF10047 inhibits glutamate release in rat cerebral cortex nerve endings. *The Journal of pharmacology and experimental therapeutics* **341**, 532-542, doi:10.1124/jpet.111.191189 (2012).
39 Meyer, D. A., Carta, M., Partridge, L. D., Covey, D. F. & Valenzuela, C. F. Neurosteroids enhance spontaneous glutamate release in hippocampal neurons. Possible role of metabotropic sigma1-like receptors. *The Journal of biological chemistry* **277**, 28725-28732, doi:10.1074/jbc.M202592200 (2002).
40 Nuwayhid, S. J. & Werling, L. L. Sigma1 receptor agonist-mediated regulation of N-methyl-D-aspartate-stimulated [3H]dopamine release is dependent

upon protein kinase C. *The Journal of pharmacology and experimental therapeutics* **304**, 364-369, doi:10.1124/jpet.102.043398 (2003).
41 Bermack, J. E. & Debonnel, G. Modulation of serotonergic neurotransmission by short- and long-term treatments with sigma ligands. *British journal of pharmacology* **134**, 691-699, doi:10.1038/sj.bjp.0704294 (2001).
42 Gonzalez-Alvear, G. M. & Werling, L. L. Sigma receptor regulation of norepinephrine release from rat hippocampal slices. *Brain research* **673**, 61-69 (1995).
43 Siniscalchi, A., Cristofori, P. & Veratti, E. Influence of N-allyl-normetazocine on acetylcholine release from brain slices: involvement of muscarinic receptors. *Naunyn-Schmiedeberg's archives of pharmacology* **336**, 425-429 (1987).
44 Soriani, O. *et al.* A-Current down-modulated by sigma receptor in frog pituitary melanotrope cells through a G protein-dependent pathway. *The Journal of pharmacology and experimental therapeutics* **289**, 321-328 (1999).
45 Zhang, H. & Cuevas, J. sigma Receptor activation blocks potassium channels and depresses neuroexcitability in rat intracardiac neurons. *The Journal of pharmacology and experimental therapeutics* **313**, 1387-1396, doi:10.1124/jpet.105.084152 (2005).
46 Wilke, R. A. *et al.* K+ channel modulation in rodent neurohypophysial nerve terminals by sigma receptors and not by dopamine receptors. *The Journal of physiology* **517 (Pt 2)**, 391-406 (1999).
47 Lupardus, P. J. *et al.* Membrane-delimited coupling between sigma receptors and K+ channels in rat neurohypophysial terminals requires neither G-protein nor ATP. *The Journal of physiology* **526 Pt 3**, 527-539 (2000).
48 Cheng, Z. X. *et al.* Neurosteroid dehydroepiandrosterone sulphate inhibits persistent sodium currents in rat medial prefrontal cortex via activation of sigma-1 receptors. *Experimental neurology* **210**, 128-136, doi:10.1016/j.expneurol.2007.10.004 (2008).
49 Gonzalez, L. G., Sanchez-Fernandez, C., Cobos, E. J., Baeyens, J. M. & del Pozo, E. Sigma-1 receptors do not regulate calcium influx through voltage-dependent calcium channels in mouse brain synaptosomes. *European journal of pharmacology* **677**, 102-106, doi:10.1016/j.ejphar.2011.12.029 (2012).
50 Tchedre, K. T. *et al.* Sigma-1 receptor regulation of voltage-gated calcium channels involves a direct interaction. *Investigative ophthalmology & visual science* **49**, 4993-5002, doi:10.1167/iovs.08-1867 (2008).
51 Ferris, C. D., Huganir, R. L., Supattapone, S. & Snyder, S. H. Purified inositol 1,4,5-trisphosphate receptor mediates calcium flux in reconstituted lipid vesicles. *Nature* **342**, 87-89, doi:10.1038/342087a0 (1989).
52 Monnet, F. P., Mahe, V., Robel, P. & Baulieu, E. E. Neurosteroids, via sigma receptors, modulate the [3H]norepinephrine release evoked by N-methyl-D-aspartate in the rat hippocampus. *Proceedings of the National Academy of Sciences of the United States of America* **92**, 3774-3778 (1995).
53 Mtchedlishvili, Z. & Kapur, J. A presynaptic action of the neurosteroid pregnenolone sulfate on GABAergic synaptic transmission. *Molecular pharmacology* **64**, 857-864, doi:10.1124/mol.64.4.857 (2003).

54 Morin-Surun, M. P., Collin, T., Denavit-Saubie, M., Baulieu, E. E. & Monnet, F. P. Intracellular sigma1 receptor modulates phospholipase C and protein kinase C activities in the brainstem. *Proceedings of the National Academy of Sciences of the United States of America* **96**, 8196-8199 (1999).
55 Kobayashi, T., Matsuno, K., Nakata, K. & Mita, S. Enhancement of acetylcholine release by SA4503, a novel sigma 1 receptor agonist, in the rat brain. *The Journal of pharmacology and experimental therapeutics* **279**, 106-113 (1996).
56 Nuwayhid, S. J. & Werling, L. L. Steroids modulate N-methyl-D-aspartate-stimulated [3H] dopamine release from rat striatum via sigma receptors. *The Journal of pharmacology and experimental therapeutics* **306**, 934-940, doi:10.1124/jpet.103.052324 (2003).
57 Zheng, P. Neuroactive steroid regulation of neurotransmitter release in the CNS: action, mechanism and possible significance. *Progress in neurobiology* **89**, 134-152, doi:10.1016/j.pneurobio.2009.07.001 (2009).
58 Hodgkin, A. L. & Huxley, A. F. A quantitative description of membrane current and its application to conduction and excitation in nerve. *The Journal of physiology* **117**, 500-544 (1952).
59 Llinas, R. & Yarom, Y. Properties and distribution of ionic conductances generating electroresponsiveness of mammalian inferior olivary neurones in vitro. *The Journal of physiology* **315**, 569-584 (1981).
60 Clapham, D. E. Calcium signaling. *Cell* **131**, 1047-1058, doi:10.1016/j.cell.2007.11.028 (2007).
61 Klette, K. L., DeCoster, M. A., Moreton, J. E. & Tortella, F. C. Role of calcium in sigma-mediated neuroprotection in rat primary cortical neurons. *Brain research* **704**, 31-41 (1995).
62 Zhang, H. & Cuevas, J. Sigma receptors inhibit high-voltage-activated calcium channels in rat sympathetic and parasympathetic neurons. *Journal of neurophysiology* **87**, 2867-2879 (2002).
63 Mayer, M. L., Westbrook, G. L. & Guthrie, P. B. Voltage-dependent block by Mg2+ of NMDA responses in spinal cord neurones. *Nature* **309**, 261-263 (1984).
64 Ishii, T. *et al.* Molecular characterization of the family of the N-methyl-D-aspartate receptor subunits. *The Journal of biological chemistry* **268**, 2836-2843 (1993).
65 Collingridge, G. L., Kehl, S. J. & McLennan, H. Excitatory amino acids in synaptic transmission in the Schaffer collateral-commissural pathway of the rat hippocampus. *The Journal of physiology* **334**, 33-46 (1983).
66 Whitlock, J. R., Heynen, A. J., Shuler, M. G. & Bear, M. F. Learning induces long-term potentiation in the hippocampus. *Science* **313**, 1093-1097, doi:10.1126/science.1128134 (2006).
67 Martina, M., Turcotte, M. E., Halman, S. & Bergeron, R. The sigma-1 receptor modulates NMDA receptor synaptic transmission and plasticity via SK channels in rat hippocampus. *The Journal of physiology* **578**, 143-157, doi:10.1113/jphysiol.2006.116178 (2007).

68 Ngo-Anh, T. J. *et al.* SK channels and NMDA receptors form a Ca2+-mediated feedback loop in dendritic spines. *Nature neuroscience* **8**, 642-649, doi:10.1038/nn1449 (2005).
69 Kim, E., Cho, K. O., Rothschild, A. & Sheng, M. Heteromultimerization and NMDA receptor-clustering activity of Chapsyn-110, a member of the PSD-95 family of proteins. *Neuron* **17**, 103-113 (1996).
70 Cui, H. *et al.* PDZ protein interactions underlying NMDA receptor-mediated excitotoxicity and neuroprotection by PSD-95 inhibitors. *The Journal of neuroscience : the official journal of the Society for Neuroscience* **27**, 9901-9915, doi:10.1523/JNEUROSCI.1464-07.2007 (2007).
71 Lin, Y., Skeberdis, V. A., Francesconi, A., Bennett, M. V. & Zukin, R. S. Postsynaptic density protein-95 regulates NMDA channel gating and surface expression. *The Journal of neuroscience : the official journal of the Society for Neuroscience* **24**, 10138-10148, doi:10.1523/JNEUROSCI.3159-04.2004 (2004).
72 Kitaichi, K. *et al.* Expression of the purported sigma(1) (sigma(1)) receptor in the mammalian brain and its possible relevance in deficits induced by antagonism of the NMDA receptor complex as revealed using an antisense strategy. *Journal of chemical neuroanatomy* **20**, 375-387 (2000).
73 Kaech, S. & Banker, G. Culturing hippocampal neurons. *Nature protocols* **1**, 2406-2415, doi:10.1038/nprot.2006.356 (2006).
74 Preibisch, S., Saalfeld, S. & Tomancak, P. Globally optimal stitching of tiled 3D microscopic image acquisitions. *Bioinformatics* **25**, 1463-1465, doi:10.1093/bioinformatics/btp184 (2009).
75 Li, Q. *et al.* A syntaxin 1, Galpha(o), and N-type calcium channel complex at a presynaptic nerve terminal: analysis by quantitative immunocolocalization. *The Journal of neuroscience : the official journal of the Society for Neuroscience* **24**, 4070-4081, doi:10.1523/JNEUROSCI.0346-04.2004 (2004).
76 Bolte, S. & Cordelieres, F. P. A guided tour into subcellular colocalization analysis in light microscopy. *Journal of microscopy* **224**, 213-232, doi:10.1111/j.1365-2818.2006.01706.x (2006).
77 Costes, S. V. *et al.* Automatic and quantitative measurement of protein-protein colocalization in live cells. *Biophysical journal* **86**, 3993-4003, doi:10.1529/biophysj.103.038422 (2004).
78 Lind, D., Franken, S., Kappler, J., Jankowski, J. & Schilling, K. Characterization of the neuronal marker NeuN as a multiply phosphorylated antigen with discrete subcellular localization. *Journal of neuroscience research* **79**, 295-302, doi:10.1002/jnr.20354 (2005).
79 Maunoury, R., Daumas-Duport, C., Fontaine, C. & Vedrenne, C. Ultrastructural localization of glial fibrillary acidic protein (GFAP) in human glioma culture by immunoperoxidase method. *Brain research* **170**, 392-398 (1979).
80 Binder, L. I., Frankfurter, A. & Rebhun, L. I. Differential localization of MAP-2 and tau in mammalian neurons in situ. *Annals of the New York Academy of Sciences* **466**, 145-166 (1986).
81 Hunt, C. A., Schenker, L. J. & Kennedy, M. B. PSD-95 is associated with the postsynaptic density and not with the presynaptic membrane at forebrain

synapses. *The Journal of neuroscience : the official journal of the Society for Neuroscience* **16**, 1380-1388 (1996).
82 Wiedenmann, B. & Franke, W. W. Identification and localization of synaptophysin, an integral membrane glycoprotein of Mr 38,000 characteristic of presynaptic vesicles. *Cell* **41**, 1017-1028 (1985).
83 JG, M. C. A New Dissection showing the Internal Gross Anatomy of the Hippocampus major. *Journal of anatomy and physiology* **33**, 76-81 (1898).
84 Sampedro, M. N., Bussineau, C. M. & Cotman, C. W. Postsynaptic density antigens: preparation and characterization of an antiserum against postsynaptic densities. *The Journal of cell biology* **90**, 675-686 (1981).
85 von Wedel, R. J., Carlson, S. S. & Kelly, R. B. Transfer of synaptic vesicle antigens to the presynaptic plasma membrane during exocytosis. *Proceedings of the National Academy of Sciences of the United States of America* **78**, 1014-1018 (1981).
86 Cui-Wang, T. *et al.* Local zones of endoplasmic reticulum complexity confine cargo in neuronal dendrites. *Cell* **148**, 309-321, doi:10.1016/j.cell.2011.11.056 (2012).
87 Cordelieres, F. P. JACoP v2.0 : improving the user experience with co-localization studies. *Interface* 174-181 (2008).
88 Hayashi, T. & Su, T. P. Intracellular dynamics of sigma-1 receptors (sigma(1) binding sites) in NG108-15 cells. *The Journal of pharmacology and experimental therapeutics* **306**, 726-733, doi:10.1124/jpet.103.051292 (2003).
89 Mavlyutov, T. A. & Ruoho, A. E. Ligand-dependent localization and intracellular stability of sigma-1 receptors in CHO-K1 cells. *Journal of molecular signaling* **2**, 8, doi:10.1186/1750-2187-2-8 (2007).
90 Beique, J. C. *et al.* Synapse-specific regulation of AMPA receptor function by PSD-95. *Proceedings of the National Academy of Sciences of the United States of America* **103**, 19535-19540, doi:10.1073/pnas.0608492103 (2006).
91 Khanna, R., Li, Q., Sun, L., Collins, T. J. & Stanley, E. F. N type Ca2+ channels and RIM scaffold protein covary at the presynaptic transmitter release face but are components of independent protein complexes. *Neuroscience* **140**, 1201-1208, doi:10.1016/j.neuroscience.2006.04.053 (2006).
92 Ossowska, K. Disturbances in neurotransmission processes in aging and age-related diseases. *Polish journal of pharmacology* **45**, 109-131 (1993).
93 Vidal, C. Nicotinic potentiation of glutamatergic synapses in the prefrontal cortex: New insight into the analysis of the role of nicotinic receptors in cognitive functions. *Drug Development Research* **31**, 120-126, doi:10.1002/ddr.430310206 (1994).
94 Maurice, T. & Privat, A. SA4503, a novel cognitive enhancer with sigma1 receptor agonist properties, facilitates NMDA receptor-dependent learning in mice. *European journal of pharmacology* **328**, 9-18 (1997).
95 Matsuno, K., Senda, T., Matsunaga, K. & Mita, S. Ameliorating effects of sigma receptor ligands on the impairment of passive avoidance tasks in mice: involvement in the central acetylcholinergic system. *European journal of pharmacology* **261**, 43-51 (1994).

96 Cummings, J. L. Alzheimer's disease. *The New England journal of medicine* **351**, 56-67, doi:10.1056/NEJMra040223 (2004).
97 Ishikawa, M. & Hashimoto, K. The role of sigma-1 receptors in the pathophysiology of neuropsychiatric diseases. *Journal of Receptor, Ligand and Channel Research* **3**, 25-36 (2010).
98 Meunier, J., Ieni, J. & Maurice, T. The anti-amnesic and neuroprotective effects of donepezil against amyloid beta25-35 peptide-induced toxicity in mice involve an interaction with the sigma1 receptor. *British journal of pharmacology* **149**, 998-1012, doi:10.1038/sj.bjp.0706927 (2006).
99 Jansen, K. L., Faull, R. L., Storey, P. & Leslie, R. A. Loss of sigma binding sites in the CA1 area of the anterior hippocampus in Alzheimer's disease correlates with CA1 pyramidal cell loss. *Brain research* **623**, 299-302 (1993).
100 Palucha, A. & Pilc, A. The involvement of glutamate in the pathophysiology of depression. *Drug news & perspectives* **18**, 262-268, doi:10.1358/dnp.2005.18.4.908661 (2005).
101 Nowak, G., Ordway, G. A. & Paul, I. A. Alterations in the N-methyl-D-aspartate (NMDA) receptor complex in the frontal cortex of suicide victims. *Brain research* **675**, 157-164 (1995).
102 Meloni, D. *et al.* Dizocilpine antagonizes the effect of chronic imipramine on learned helplessness in rats. *Pharmacology, biochemistry, and behavior* **46**, 423-426 (1993).
103 Kelly, J. P., Wrynn, A. S. & Leonard, B. E. The olfactory bulbectomized rat as a model of depression: an update. *Pharmacology & therapeutics* **74**, 299-316 (1997).
104 Wang, D. *et al.* Role of N-methyl-D-aspartate receptors in antidepressant-like effects of sigma 1 receptor agonist 1-(3,4-dimethoxyphenethyl)-4-(3-phenylpropyl)piperazine dihydrochloride (SA-4503) in olfactory bulbectomized rats. *The Journal of pharmacology and experimental therapeutics* **322**, 1305-1314, doi:10.1124/jpet.107.124685 (2007).
105 Rowland, L. P. & Shneider, N. A. Amyotrophic lateral sclerosis. *The New England journal of medicine* **344**, 1688-1700, doi:10.1056/NEJM200105313442207 (2001).
106 Al-Saif, A., Al-Mohanna, F. & Bohlega, S. A mutation in sigma-1 receptor causes juvenile amyotrophic lateral sclerosis. *Annals of neurology* **70**, 913-919, doi:10.1002/ana.22534 (2011).
107 Cobos, E. J., Entrena, J. M., Nieto, F. R., Cendan, C. M. & Del Pozo, E. Pharmacology and therapeutic potential of sigma(1) receptor ligands. *Current neuropharmacology* **6**, 344-366, doi:10.2174/157015908787386113 (2008).

1)